第42卷 第1期 岩 石 矿 物 学 杂 志 Vol. 42, No. 1: 83~103
2023年1月 ACTA PETROLOGICA ET MINERALOGICA Jan., 2023

四川盆地西缘上二叠统宣威组顶部泥岩、砂岩的地球化学特征及其地质意义

詹宏宇[1],何 青[1],曾方侣[2],邓煜霖[1],王旭辉[1],李 亮[3],娄渝明[1],谢富伟[1],王 勇[1],郎兴海[1]

(1. 成都理工大学 地球科学学院, 四川 成都 610059; 2. 中建八局西南公司 基础设施分公司, 四川 成都 610041; 3. 四川省华地建设工程有限责任公司, 四川 成都 610036)

摘 要:沉积物源分析是认识盆山演化的重要途径。了解四川盆地西南缘上二叠统宣威组物源,对于重建晚二叠世扬子克拉通周缘演化具有重要意义。本文对峨眉山地区宣威组顶部泥岩、砂岩开展了岩石学和全岩地球化学分析,进行了物源、沉积环境和构造背景的研究。宣威组泥岩主要成分为黏土矿物,SiO_2 含量(平均 49.42%)中等;砂岩成分大部分为火山岩屑,含有少量石英及长石,具中等的 SiO_2 含量(平均 44.12%),属于杂砂岩系列。泥岩与砂岩均具有轻稀土元素富集、重稀土元素较右倾的稀土元素配分型式,微量元素相对大陆上地壳富集高场强元素(如 Nb、Zr),亏损大离子亲石元素(如 Sr、Ba)。根据地球化学分析结果结合已发表的扬子克拉通周缘二叠系沉积岩数据,认为上二叠统宣威组顶部沉积岩物源区经历了强烈的化学风化作用,沉积古环境为富氧的淡水沉积环境;宣威组顶部沉积物物源不仅来自于近源搬运的峨眉山高 Ti 玄武岩,还接受了扬子克拉通的补给,扬子克拉通西缘晚二叠世时期是活动大陆边缘沉积。

关键词:扬子克拉通;晚二叠世;峨眉山大火成岩省;全岩地球化学;宣威组

中图分类号:P588.2;P542 **文献标识码**:A **文章编号**:1000-6524(2023)01-0083-21

Geochemical characteristics and geological implications of mudstones and sandstones at the top of the Upper Permian Xuanwei Formation on the western margin of Sichuan Basin

ZHAN Hong-yu[1], HE Qing[1], ZENG Fang-lü[2], DENG Yu-lin[1], WANG Xu-hui[1], LI Liang[3], LOU Yu-ming[1], XIE Fu-wei[1], WANG Yong[1] and LANG Xing-hai[1]

(1. College of Geosciences, Chengdu University of Technology, Chengdu 610059, China; 2. Infrastructure Branch, China Construction Eighth Bureau Southwest Company, Chengdu 610041, China; 3. Sichuan Huadi Construction Engineering Co., Ltd, Chengdu 610036, China)

Abstract: Provenance analysis is an important way to understand basin mountain evolution. Understanding the provenance of the Upper Permian Xuanwei Formation in the southwest margin of Sichuan Basin is of great significance for reconstructing the evolution of the Late Permian Yangtze Craton perimeter. In this paper, the petrology and whole-rock geochemical analyses of mudstone and sandstone at the top of Xuanwei Formation in the Emeishan area are analyzed, and the provenance, sediment environment and tectonic setting are studied. The mudstone of the

收稿日期:2022-07-12;**接受日期**:2022-10-09;**编辑**:郝艳丽

基金项目:四川省科技计划项目(2020JDJQ0042);成都理工大学珠峰科学研究计划(2020ZF11407)

作者简介:詹宏宇(1997-),男,硕士生,主要从事地质学基础研究,E-mail:m13990526329@163.com;通讯作者:郎兴海(1982-)男,博士,教授,长期从事找矿勘查与矿床学研究,E-mail:langxinghai@126.com。

网络首发时间:2022-12-26;**网络首发地址**:https://kns.cnki.net/kcms/detail/11.1966.P.20221223.1419.001.html

Xuanwei Formation is mainly composed of clay minerals with medium SiO_2 content (average 49.42%); the sandstone is mostly composed of volcanic rock fragments, containing a small amounts of quartz and feldspar, with medium SiO_2 content (average 40.12%), belonging to the greywacke series. Mudstone and sandstone of Xuanwei Formation have light rare earth element enrichment, heavier rare earth elements are more right-leaning. Compared with the continental upper crust, trace elements are relatively rich in high field strength elements (such as Nb, Zr) and relatively depleted in large ion lithophile elements (such as Sr, Ba). Combined with the published data of Permian sediments at the perimeter of the Yangtze Craton, it is considered that the source area of sediments at the top of Permian Xuanwei Formation experienced strong chemical weathering, and the depositional paleoenvironment was an oxygen-rich freshwater environment. The sediments at the top of Xuanwei Formation not only came from the Emeishan high-Ti basalt transported near the source, but also supplied by the Yangtze Craton. The western margin of the Yangtze Craton was deposited on the active continental margin during the Late Permian.

Key words: Yangtze Craton; Late Permian; Emeishan large igneous province; whole-rock geochemistry; Xuanwei Formation

Fund support: Sichuan Science and Technology Program (2020JDJQ0042); Everest Scientific Research Program of Chengdu University of Technology (2020ZF11407)

二叠纪中晚期,我国西南地区发生了规模巨大的岩浆喷溢事件,形成了著名的峨眉山大火成岩省(Chung and Jahn, 1995; Courtillot *et al.*, 1999; 张招崇, 2009; 徐义刚等, 2013),它的形成直接影响了我国西南地区的海陆演变(Chen *et al.*, 2003)、沉积(He *et al.*, 2003, 2005, 2007; 梁狄刚等, 2009; 陈宗清, 2011; 赵宗举等, 2012; 徐义刚等, 2013; 张天福等, 2016; 马骏等, 2017; 焦鑫等, 2017; 田野, 2018; 陈建平等,2018; 蒋晓丽等, 2022)及成藏成矿作用(Ali *et al.*, 2005; 张招崇, 2009),甚至可能引发了二叠纪全球性气候变化和生物大灭绝事件(胡瑞忠等, 2005; 赖旭龙等, 2009; 朱江等, 2011),因此成为了国内外关注的热点地区(Ukstins Peate and Bryan, 2008; Shellnutt, 2014; Zhu *et al.*, 2018, 2019, 2021; Zhang *et al.*, 2020; Huang *et al.*, 2022)。近年来,对晚二叠世的沉积地层研究取得了很多进展,不少学者对川滇黔地区分布的上二叠统沉积岩开展了沉积环境、构造环境、物源分析以及成矿意义等方面的研究(He *et al.*, 2007; Zhang *et al.*, 2010; Zhao *et al.*, 2016; 何冰辉等, 2017; 张廷山等, 2017),但关于上二叠统沉积岩的物源仍存在较大分歧。目前针对上二叠统沉积岩的物源有单一物源和混合物源两种观点。前者认为物源来自峨眉山大火成岩省,其证据主要来自城口巫溪地区上二叠统吴家坪组(P_3w)的碎屑锆石年龄(梁新权等, 2013)、四大寨晒瓦组(P_3s)沉积岩的地球化学特征(Yang *et al.*, 2015)、黔西南地区上二叠统龙潭组(P_3l)的地球化学特征(于鑫等, 2017)以及右江盆地北缘上二叠统龙潭组(P_3l)泥岩和砂岩的地球化学和锆石年代学数据(邓旭升, 2019)。后者认为物源来自峨眉山大火成岩省及扬子克拉通西南缘,其中Xu等(2001)和Ali等(2005)认为峨眉山大火成岩省主要由玄武岩组成,无法提供大量的碎屑锆石;何冰辉(2015)对宣威组下部地层的碎屑锆石进行的LA-ICP-MS U-Pb研究认为扬子克拉通西南缘在晚二叠世为宣威组提供了大量的物质来源;何冰辉等(2017)通过对滇东者海宣威组下部地层的碎屑锆石特征、稀土元素的研究,推测扬子克拉通西南缘为宣威组提供了部分碎屑物源。因此,对宣威组泥岩及砂岩进行全岩地球化学,并结合区域二叠纪沉积岩的地球化学数据综合研究,有助于判断上二叠统沉积岩的物源,并约束其沉积环境,理解扬子克拉通西缘晚二叠世构造演化。

本文以四川盆地西缘峨眉山地区宣威组顶部的砂岩、泥岩为研究对象,开展了沉积岩岩石学、地球化学分析,并结合前人的研究成果,约束宣威组的物源属性、沉积古环境及沉积构造背景,对理解扬子克拉通西南缘的演化具有重要意义。

1 区域地质背景

四川盆地处于扬子克拉通西侧,是由北东与北西向交叉的深断裂活动形成的菱形构造沉积盆地,为扬子克拉通的一个次级构造单元(朱志军等,

2012；罗宏谓，2019）。四川盆地北邻秦岭造山带，西邻龙门造山带和松潘-甘孜褶皱带，东面为华南褶皱带。四川盆地属内陆多旋回盆地，在印支期受挤压作用形成了盆地雏形，后遭受了一系列喜马拉雅期强烈的压扭性断褶活动，形成了现今盆地的构造面貌（图 1，林茂炳，1994；刘和甫等，1994；郑荣才等，2009）。四川盆地是在扬子克拉通基础上经多期构造旋回形成和发展起来的复合型或叠合型盆地（张岳桥等，2011），盆地基底为前震旦系的变质结晶基底，经历了中元古代（1.8～1.0 Ga）多次地壳增生作用后，最后由晋宁运动（1 000～830 Ma）固结形成（Chen and Jahn，1998；Qiu *et al.*，2000；陆松年等，2004；Zheng *et al.*，2006）。盆地还经历了震旦纪-中三叠世的海相碳酸盐岩台地、晚三叠世-始新世的陆相碎屑盆地和渐新世以来的构造盆地 3 大演化阶段（汪泽成，2002；刘树根等，2011）。古生代以后四川盆地西缘处于被动大陆边缘环境（汪泽成，2002），直到晚三叠世古特提斯洋向东逐渐闭合，松潘甘孜地区被挤压形成褶皱，龙门山开始早期隆升，扬子西缘的四川盆地也由被动大陆边缘转为前陆盆地（陈斌等，2016）。

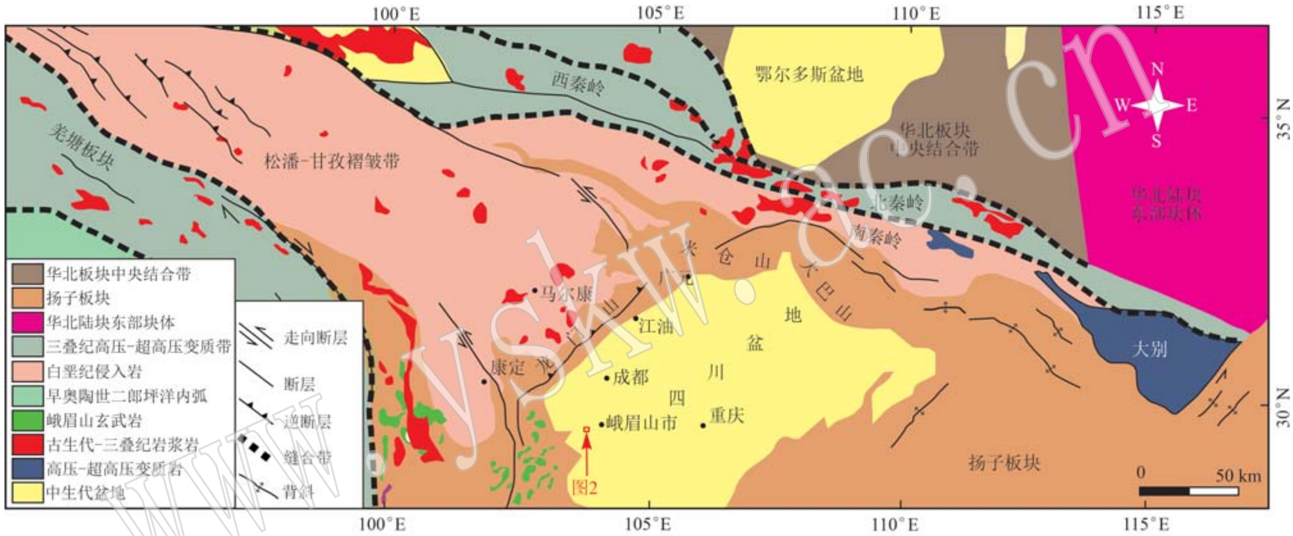

图 1　四川盆地及邻区构造背景图（据 Enkelmann *et al.*，2007；邓煜霖等，2018；李宸等，2020）

Fig. 1　Tectonic setting of Sichuan Basin and adjacent regions (after Enkelmann *et al.*, 2007; Deng Yulin *et al.*, 2018; Li Chen *et al.*, 2020)

峨眉山地区位于四川盆地的西缘（图 1）。震旦纪-三叠纪末，四川盆地整体处于被动大陆边缘环境，主要沉积以碳酸盐岩、泥岩及砂岩为主的地层（曾允孚等，1979；庞攀，2015；王贝，2017；耿元生等，2017；陈风霖等，2018；张浩然等，2020）。二叠纪末，四川盆地主体主要沉积一套硅质灰岩组合的吴家坪组、长兴组及硅质砂页岩组合的大隆组，而盆地西南受峨眉山地幔柱活动的影响，主要沉积以砂岩为代表的河流相宣威组及海陆交互相的成煤岩系龙潭组（马永生，2009；邵龙义等，2013）。三叠纪的印支运动主要表现为升降运动，三叠纪初期为河流环境（冯冲等，2015），晚三叠世地壳沉降，形成了浅海沉积环境（余世花，2016）。早侏罗世至中侏罗世早期，地壳继续沉降，由河流环境转变为内陆湖泊环境。新近纪至第四纪，峨眉山地区抬升隆起，缺失了中新世沉积，形成了中更新统与下伏上新统间的不整合面（陈璐，2014）。

峨眉山地区主要分布上元古界至第四系的地层，除泥盆系、志留系、石炭系以及奥陶系中、上统地层缺失外，其他时代地层出露相对较为完整（图 2）（张继庆，1983；Dong *et al.*，2006；黄丹，2012；庞攀，2015；姚婕，2018），其中宣威组（P_3x）是一套杂色砂岩、粉砂岩、泥岩及煤线的旋回层，底部为玄武岩的古风化壳，与下伏峨眉山玄武岩（P_3e）平行不整合接触。上覆地层为东川组（T_1d），主要为紫红色砂岩、粉砂岩及泥岩的旋回层。峨眉山地区岩浆岩主要由新元古代峨眉山花岗岩及晚二叠世峨眉山玄武岩构成（图 1）（庞攀，2015；姚婕，2018；Zhu *et al.*，2019）。

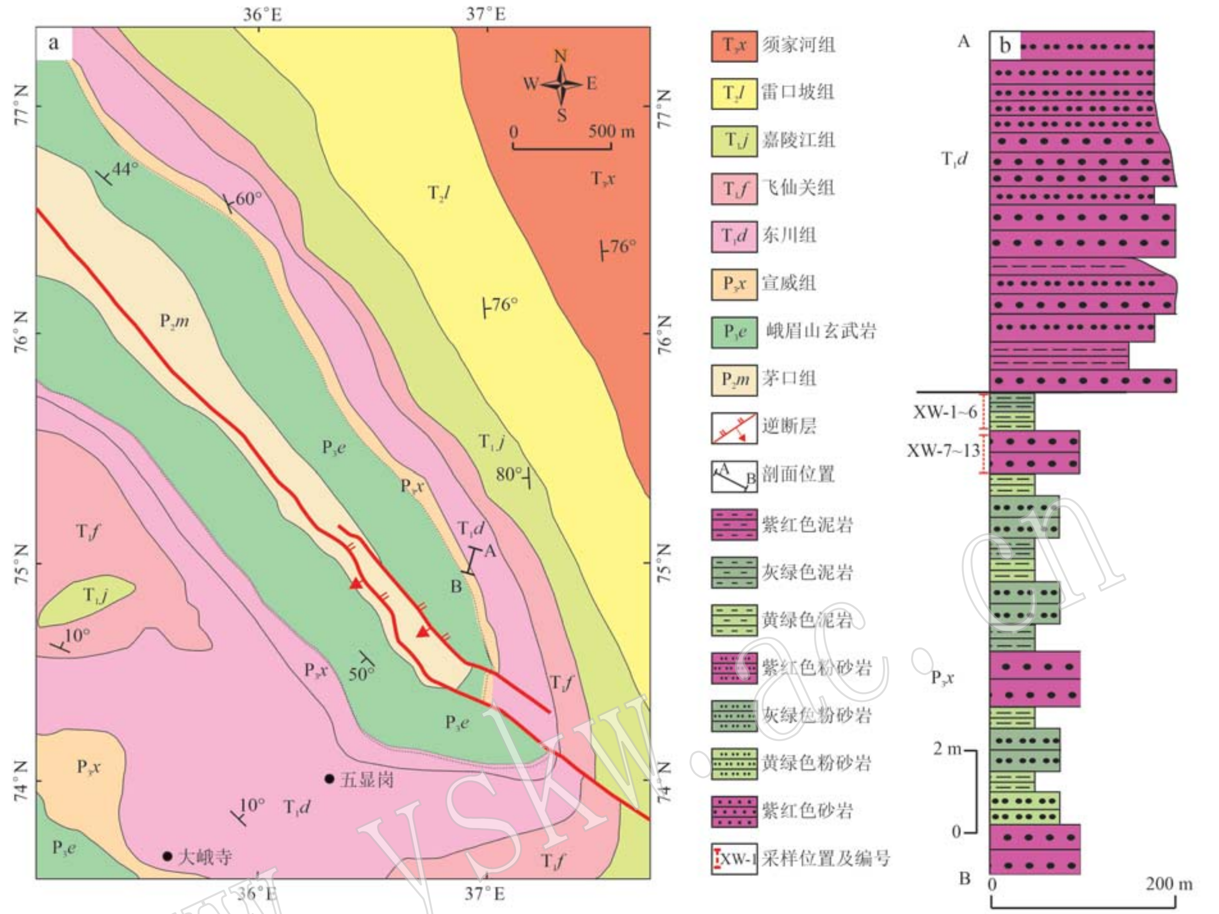

图 2　研究区地质简图(a,据李宸等, 2020)和峨眉山地区宣威组-东川组地层柱状图(b)

Fig. 2　Sketch geological map of the study area (a, after Li Chen *et al.*, 2020) and the simplified stratigraphic column of the Xuanwei-Dongchuan Formations in the Emeishan area(b)

2　样品采集及测试方法

样品采集自四川峨眉山地区的宣威组(P_3x)顶部(图 2b),坐标 N29°34′52″、E103°24′50″。本次样品主要采自风化程度较弱的新鲜岩石,13 件样品中泥岩样品有 6 件(XW-1~XW-6),砂岩样品有 7 件(XW-7~XW-13)。泥岩呈灰绿、黄绿色,含粉砂黏土结构,薄层状构造(图 3a),镜下可见主要成分为高岭石等黏土矿物,含少量石英,局部可见海绿石、绿泥石(图 3c)。砂岩呈紫红色,不等粒砂状结构,中-薄层状构造(图 3b),镜下可见成分大部分为火山岩屑,含有少量石英及长石,局部可见海绿石,胶结物主要为铁质(图 3d)。

样品的全岩主微量、稀土元素分析在西南冶金地质测试中心进行。样品去除风化面后,用自来水清洗后分别用 5% HNO_3 和 5% HCl 在超声波清洗仪中浸泡至无气泡产生,再用纯净水把样品冲洗干净,在低于 100℃环境中烘干,在确保样品不会相互污染的情况下,将样品细碎到 200 目筛孔以下进行分析测试。常量元素测试采用 X 射线荧光光谱法(XRF),在荷兰帕纳科 Axios X 荧光仪下完成,分析误差优于 3%。称取 0.1~0.5 g 全岩粉末样品置于聚四氟坩埚中,用氢氟酸和硫酸进行分析,用重铬酸钾标准溶液滴定得到 FeO 含量,换算后,用 XRF 法获得的 $^{T}Fe_2O_3$ 含量减去 FeO 含量,得到 Fe_2O_3 含量。微量元素和稀土元素测定采用电感耦合等离子体质谱法(ICP-MS),在 NexIon 300x ICP-MS 仪器上完成,将细碎好的样品用酸溶法制成溶液,然后在等离子质谱仪上进行测定,并用标准溶液进行校正,实验具体方法步骤据参考文献(Qi *et al.*, 2000),含量大于 10×10^{-6} 元素分析误差小于 5%,含量小于 10×10^{-6} 的元素误差小于 10%。

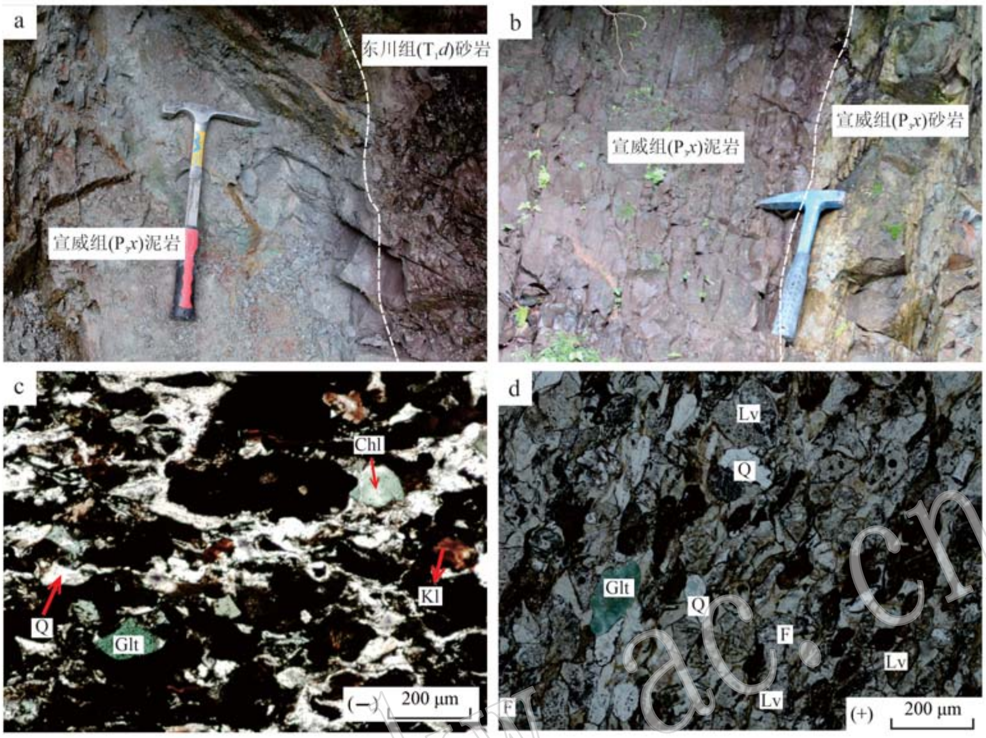

图 3　峨眉山地区宣威组顶部泥岩和砂岩野外露头(a、b)和显微镜下照片(c、d)

Fig. 3　Field photos(a, b) and microscopic photos (c, d) of the mudstone and sandstone at the top of the Xuanwei Formation in the Emeishan area

Q—石英；F—长石；Lv—火山岩屑；Glt—海绿石；Kl—高岭石；Chl—绿泥石

Q—quartz；F—feldspar；Lv—volcanic rock fragments；Glt—glauconite；Kl—kaolinite；Chl—chlorite

3　分析结果

3.1　主量元素

宣威组顶部 6 件泥岩样品及 7 件砂岩样品的常量元素分析结果见表 1。泥岩 SiO_2 含量为 47.52%~51.65%,平均为 49.42%;Al_2O_3 含量为 18.67%~19.52%,平均为 19.11%;MnO 和 Fe_2O_3 含量较低,分别为 0.10%~0.13%和 1.11%~1.71%。其余常量元素含量分别为 TiO_2(2.82%~3.07%)、K_2O(2.98%~3.30%)、FeO(6.73%~9.02%)和 P_2O_5(0.18%~0.35%)、MgO(2.04%~2.48%)、Na_2O(0.01%~0.04%)以及 CaO(0.66%~0.83%)。较低的 CaO 含量及烧失量(LOI=7.24%~7.41%)表明黏土矿物及碳酸盐矿物含量较少,这与镜下观察到的现象是一致的(图 3c)。

宣威组顶部砂岩具有较低的 SiO_2 含量,范围为 39.60%~40.50%,平均为 44.12%;较高的 Fe_2O_3 含量,为 17.15%~18.59%;Al_2O_3 含量为 18.96%~19.67%,平均为 19.3%;其余常量元素含量分别为 TiO_2(3.63%~4.11%)、K_2O(3.10%~3.25%)、P_2O_5(0.24%~0.27%)、FeO(3.93%~4.80%)、Na_2O(0.08%~0.11%)、MgO(1.59%~1.65%)、CaO(0.88%~0.93%)以及 MnO(0.06%~0.07%)。与泥岩样品相比,砂岩样品明显受到淋滤作用影响,CaO 含量明显降低,K_2O 含量却较高(表 1)。在 lg(K_2O/Na_2O)-lg(SiO_2/Al_2O_3)砂岩分类图解上,砂岩样品均位于杂砂岩区域内(图 4)。

3.2　稀土、微量元素特征

宣威组顶部泥岩和砂岩样品的稀土、微量元素含量及特征见表 2。泥岩的 ΣREE 为 164.74×10^{-6}~$2\,824.74\times10^{-6}$,平均为 $1\,110.77\times10^{-6}$; LREE 为 144.92×10^{-6}~$2\,646.34\times10^{-6}$,平均为 $1\,022.63\times10^{-6}$;HREE 为 19.82×10^{-6}~178.40×10^{-6},平均为 88.14×10^{-6};轻稀土元素与重稀土元素分馏较为明显,LREE/HREE 为 5.31~14.83,平均 9.71,$(La/Yb)_N$ 值为 4.13~23.97,平均为 11.89;δCe 值为 0.93~2.35,平均为 1.48;δEu 值为 0.33~0.61(除 XW04 为 1.07

表 1 峨眉山地区宣威组顶部泥岩、砂岩主量元素分析结果 $w_B/\%$

Table 1 Analytical results of major elements contents of mudstone and sandstone samples at the top of the Xuanwei Formation in the Emeishan area

样品	泥岩						砂岩						
岩性	XW-1	XW-2	XW-3	XW-4	XW-5	XW-6	XW-7	XW-8	XW-9	XW-10	XW-11	XW-12	XW-13
SiO_2	50.38	48.11	47.52	51.65	49.26	49.30	40.24	40.32	40.50	39.95	40.44	39.95	39.60
Al_2O_3	19.35	18.67	19.52	19.26	19.15	18.75	19.21	19.48	19.40	18.96	19.67	19.25	19.11
Fe_2O_3	1.62	1.19	1.51	1.61	1.11	1.71	17.79	17.15	17.57	18.05	17.71	17.84	18.59
FeO	7.80	8.22	9.01	6.73	9.02	7.71	4.10	4.37	4.22	4.80	3.93	4.24	3.93
MgO	2.48	2.25	2.34	2.04	2.30	2.17	1.59	1.62	1.61	1.65	1.59	1.63	1.59
CaO	0.75	0.83	0.74	0.66	0.74	0.68	0.90	0.89	0.88	0.90	0.90	0.91	0.93
Na_2O	0.02	0.01	0.01	0.04	0.02	0.03	0.09	0.08	0.09	0.09	0.09	0.11	0.09
K_2O	3.30	2.98	3.15	3.30	3.12	3.13	3.22	3.21	3.19	3.10	3.25	3.19	3.13
TiO_2	3.00	3.07	3.05	2.82	3.04	2.96	3.74	3.63	3.70	3.88	3.73	3.89	4.11
MnO	0.11	0.12	0.12	0.10	0.13	0.11	0.06	0.07	0.07	0.07	0.06	0.07	0.07
P_2O_5	0.26	0.35	0.28	0.18	0.27	0.24	0.25	0.24	0.24	0.26	0.24	0.26	0.27
LOI	7.41	7.25	7.38	7.33	7.24	7.25	8.24	8.31	8.01	7.87	7.81	8.08	8.14
CaO^*	0.01	0.01	0.01	0.04	0.02	0.03	0.09	0.08	0.09	0.09	0.09	0.11	0.09
CIA	85.30	86.17	86.03	85.06	85.85	85.44	84.96	85.25	85.20	85.25	85.15	84.95	85.24
ICV	0.54	0.52	0.52	0.52	0.51	0.54	1.38	1.33	1.36	1.42	1.35	1.39	1.45
PIA	99.79	99.89	99.88	99.48	99.78	99.58	98.89	99.03	98.90	98.88	98.92	98.65	98.89

外),平均为0.60,有明显的负Eu异常。从稀土元素配分模式图中可以看出,宣威组泥岩具有轻稀土元素富集、重稀土元素较右倾、具Eu负异常的特点(图5a),这些特征与峨眉山玄武岩相似。泥岩的微量元素含量与大陆上地壳(UCC)相比(Rudnick and Gao, 2003),高场强元素(如Nb、Zr、Pb等)相对富集,大离子亲石元素(如Sr、Ba)出现强烈的亏损(图5b)。

砂岩的ΣREE为$170.88\times10^{-6}\sim361.52\times10^{-6}$,平均为$259.18\times10^{-6}$;LREE为$149.18\times10^{-6}\sim317.66\times10^{-6}$,平均为$225.29\times10^{-6}$; HREE为$21.70\times10^{-6}\sim43.86\times10^{-6}$,平均为$33.89\times10^{-6}$;轻稀土元素与重稀土元素含量差异较大,分馏较为明显,LREE/HREE与$(La/Yb)_N$值均较高,LREE/HREE值为5.25~7.26,平均为6.43,$(La/Yb)_N$值为3.65~12.97,平均为8.53;δCe值为0.72~1.84,平均为1.12;δEu值为1.11~1.33,平均为1.2,表明有弱的正Eu异常。从稀土元素配分模式图中可以看出,宣威组砂岩具有轻稀土元素富集、重稀土元素较右倾、具Eu正异常、Ce微弱异常的特点,这些特征与峨眉山玄武岩相似(图5a)。砂岩的微量元素含量与大陆上地壳(UCC)(Rudnick and Gao, 2003)相比,相对富集高场强元素(如Nd、Zr、Hf等),相对亏损大离子亲石元素(如Sr、Ba等)(图5b)。

4 讨论

4.1 物源区的古风化条件

湿润气候条件下,化学风化作用占主导地位,强烈控制碎屑岩的主量元素和微量元素组成(Nesbitt and Young, 1982; McLennan *et al.*, 1993; Fedo *et al.*, 1995)。相反,在干旱气候下,物理风化占主导地位,岩石化学成分不会发生重大变化。因此,化学指标为物源区古风化提供了一种良好的手段。在Al_2O_3-($CaO+Na_2O$)-K_2O(A-CN-K)三元图中,样品偏离了钾交代作用趋势线(蓝色实线箭头)(Fedo *et al.*, 1995),而位于预测的理想风化趋势(红色实线箭头)的顶部,暗示了较强的风化作用(图6a)。这种强烈的风化作用可能导致了K_2O的降低,从而提高了宣威组样品的化学蚀变指数CIA值(84.95~86.17,平均85.40,图6a),表明样品经历了较强烈的风化作用(Nesbitt and Young, 1982)。所有的样品都位于斜长石与钾长石连线(灰色实线)之上,也表明这些样品在源区经历了强烈的风化作用。此外,宣威组样品中大量的高岭石可能来自宣威组泥岩及砂岩中长石的风化,也支持了强烈风化作用(图3c、3d)。同时,斜长石蚀变指数(PIA值)(98.65~99.89,平均99.27,表1)也表明物源经历了强烈的

表 2　峨眉山地区宣威组顶部泥岩、砂岩微量元素和稀土元素分析结果　$w_B/10^{-6}$

Table 2　Analytical results of trace elements and REE contents of mudstone and sandstone samples at the top of the Xuanwei Formation in the Emeishan area

样品编号	泥岩						砂岩						
	XW-1	XW-2	XW-3	XW-4	XW-5	XW-6	XW-7	XW-8	XW-9	XW-10	XW-11	XW-12	XW-13
La	60.00	66.60	66.10	58.30	61.70	64.50	46.95	48.81	49.91	45.87	46.73	40.35	41.39
Ce	112.00	129.00	119.00	107.00	112.00	121.00	114.70	121.40	122.70	115.30	116.90	107.50	105.10
Pr	15.00	17.70	15.60	14.10	14.60	15.90	15.42	16.17	16.08	15.40	15.92	14.98	14.31
Nd	54.30	68.00	53.90	49.20	50.50	56.70	65.88	68.82	69.48	66.24	68.34	66.07	62.79
Sm	9.46	12.90	9.11	7.62	8.52	9.47	15.24	16.12	16.44	15.74	16.08	16.15	15.34
Eu	2.14	3.07	2.12	1.75	1.96	2.20	4.28	4.49	4.59	4.38	4.57	4.46	4.27
Gd	7.68	10.47	7.74	6.46	7.08	7.79	11.42	11.83	12.21	11.61	11.93	11.79	11.28
Tb	1.25	1.63	1.24	1.06	1.13	1.27	1.96	2.01	2.09	1.99	2.07	2.05	1.94
Dy	6.40	7.90	6.54	5.76	5.91	6.60	9.25	9.32	9.92	9.43	9.72	9.73	9.35
Ho	1.24	1.50	1.27	1.18	1.15	1.29	1.60	1.60	1.77	1.60	1.69	1.65	1.59
Er	3.18	3.77	3.38	3.11	3.00	3.33	3.81	3.71	4.18	3.70	4.07	3.96	3.72
Tm	0.46	0.52	0.49	0.45	0.43	0.48	0.56	0.55	0.62	0.54	0.61	0.57	0.58
Yb	2.69	2.94	2.87	2.72	2.53	2.76	3.11	3.06	3.54	3.07	3.35	3.13	3.22
Lu	0.41	0.45	0.43	0.41	0.39	0.42	0.45	0.43	0.52	0.45	0.50	0.45	0.45
Y	31.10	36.60	32.40	30.00	29.80	32.50	35.75	35.63	39.62	35.34	38.28	37.10	36.03
As	0.23	0.44	0.62	0.34	1.43	1.43	0.82	0.68	2.76	0.65	0.68	0.44	0.45
Cd	0.06	0.06	0.05	0.15	0.27	0.07	0.15	0.03	0.03	0.02	0.03	0.02	0.04
Co	98.39	96.00	98.65	88.12	105.41	92.27	52.43	53.48	53.89	53.17	51.27	52.81	51.57
Cr	150.39	156.08	151.78	150.08	150.20	150.57	324.19	330.83	335.36	364.10	330.44	366.33	387.51
Zn	210.98	212.35	222.82	204.11	267.00	217.18	165.75	138.10	135.60	142.15	122.90	135.90	137.90
Ga	30.71	28.37	30.33	28.95	31.00	29.91	36.17	36.69	35.79	33.72	35.84	35.91	33.63
Ge	1.37	1.30	1.34	1.29	1.43	1.33	1.73	1.59	1.79	1.61	1.65	1.75	1.70
Mo	0.36	0.33	0.35	0.33	0.43	0.34	9.90	2.78	2.08	1.06	1.34	0.99	0.73
Nb	36.15	35.33	36.07	34.43	37.81	36.22	21.30	20.94	20.95	21.43	21.39	21.62	22.13
Ni	133.08	123.62	132.93	124.81	138.52	123.93	155.38	161.51	158.24	151.94	156.89	167.88	165.61
Rb	104.30	94.36	101.94	105.19	100.73	100.61	83.05	84.73	82.82	82.14	84.41	84.72	82.40
Sb	0.07	0.07	0.10	0.06	0.33	0.11	1.05	0.78	11.58	0.52	0.59	0.42	0.38
Sc	29.66	29.35	29.08	28.33	30.40	30.43	41.20	41.19	40.74	39.49	41.24	40.68	38.92
Se	0.04	0.04	0.04	0.06	0.04	0.03	0.13	0.14	0.14	0.11	0.13	0.12	0.11
Sn	3.96	3.56	3.68	3.50	3.77	3.56	3.25	2.94	2.92	2.87	2.73	2.70	2.96
Sr	58.86	61.57	57.95	64.31	57.39	57.89	95.67	100.22	98.51	94.12	95.78	102.59	93.06
Zr	393.48	400.38	407.23	392.56	406.27	397.94	322.17	312.92	315.16	316.02	321.72	321.40	324.12
Te	0.04	0.04	0.04	0.04	0.06	0.06	0.02	0.02	0.02	0.02	0.02	0.02	0.02
Tl	0.54	0.65	0.43	0.42	0.42	0.48	0.31	0.30	0.29	0.31	0.29	0.29	0.27
V	281.75	306.61	295.00	291.61	288.22	295.87	446.30	441.90	425.90	439.85	404.80	441.30	425.70
Cs	2.87	2.28	2.69	2.51	2.77	2.59	1.78	1.63	1.62	1.56	1.71	1.73	1.56
Ba	288.33	304.32	297.14	311.72	300.91	305.47	460.30	451.80	429.20	420.75	421.90	441.60	436.90
Hf	28.07	37.85	32.62	24.60	28.40	31.99	7.76	7.76	7.70	7.66	7.99	7.81	7.81
Ta	2.87	2.78	2.86	2.76	2.97	2.83	2.73	2.62	2.58	1.78	2.64	2.69	1.63
W	1.19	0.99	0.90	0.99	1.31	0.92	0.78	0.90	0.63	0.44	0.61	0.66	0.31
Pb	4.76	5.62	5.70	37.73	100.09	9.59	19.82	16.72	15.41	16.23	15.60	19.49	15.53
Bi	0.11	0.08	0.08	0.09	0.12	0.17	0.20	0.13	0.15	0.13	0.12	0.12	0.11
Th	5.23	4.23	4.26	3.60	4.34	4.21	6.06	5.54	5.66	5.59	5.74	5.81	5.36
U	1.45	1.17	1.06	1.08	1.15	1.14	1.47	1.23	1.22	1.25	1.30	1.24	1.20
ΣREE	754.98	2 824.74	874.16	164.74	412.36	865.67	195.73	322.22	361.52	291.30	232.18	226.43	170.88
LREE	644.41	2 646.34	808.96	144.92	346.96	798.15	164.39	279.48	317.66	256.03	201.20	192.84	149.18
HREE	110.57	178.40	65.20	19.82	65.40	67.52	31.34	42.74	43.86	35.27	30.98	33.59	21.70
LREE/HREE	5.83	14.83	12.41	7.31	5.31	11.82	5.25	6.54	7.24	7.26	6.49	5.74	6.87
$(La/Yb)_N$	4.13	23.97	13.88	5.63	4.91	14.46	3.65	8.28	10.85	12.97	7.65	7.38	9.34
δEu	0.35	0.33	0.51	1.07	0.54	0.61	1.20	1.33	1.11	1.14	1.20	1.21	1.17
δCe	2.35	1.07	1.35	1.44	1.39	0.93	1.84	1.02	0.72	0.83	1.08	1.01	1.02

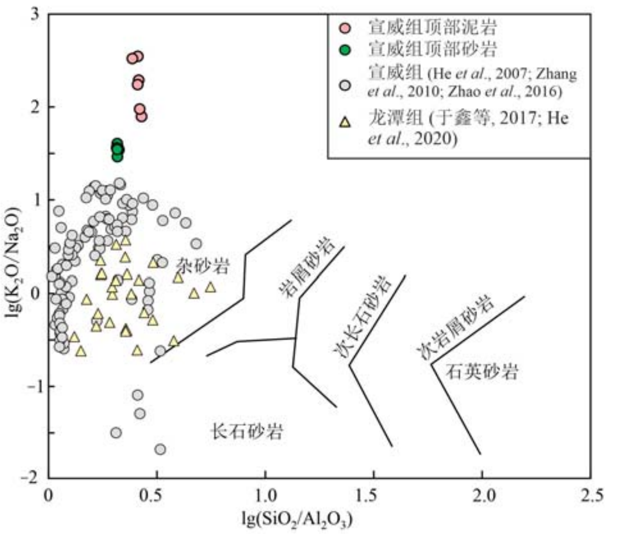

图 4 峨眉山地区宣威组沉积岩岩石分类命名图解（底图据 Pettijohn *et al.*, 1987）

Fig. 4 Illustration of rock classification of Xuanwei Formation sediments in the Emeishan area (after Pettijohn *et al.*, 1987)

化学风化(Fedo *et al.*, 1995)。对于成分变异性指数 ICV(Cox *et al.*, 1995)，泥岩样品的值为 0.51～0.54(强烈风化)，砂岩样品的值为 1.33～1.45(中等风化)，这些数值表明在半湿到潮湿的条件下，物源存在中度到强烈的化学风化(Ivanova *et al.*, 2015)。

运输过程中的水力分选主要是对矿物成分(Al_2O_3、TiO_2 和 SiO_2)进行分选，因此限制了物源的组成(Garcia *et al.*, 1991)。在 Al_2O_3-Zr-TiO_2 三元相图上(图 6b)，样品具有低的 Zr 和相对较高的 Al_2O_3 和 TiO_2 含量，表明分选过程较弱。微量元素比值也常用来确定源区的风化作用，宣威组样品在 Th/Sc-Zr/Sc 双变量图上沿着组分变化的趋势分布(图 6c，McLennan *et al.*, 1993)，表明沉积岩主要受组分变化控制，而不是水力分选。同时，在半湿到潮湿的环境中的风化作用主要以氧化反应为主，在这个过程中，一些元素，如 U^{4+} 被氧化(U^{4+} 到 U^{6+})通过淋滤作用消除，而不是 Th 残留在未风化的残留物中(McLennan and Taylor, 1980)，因此沉积岩的 Th/U 值与

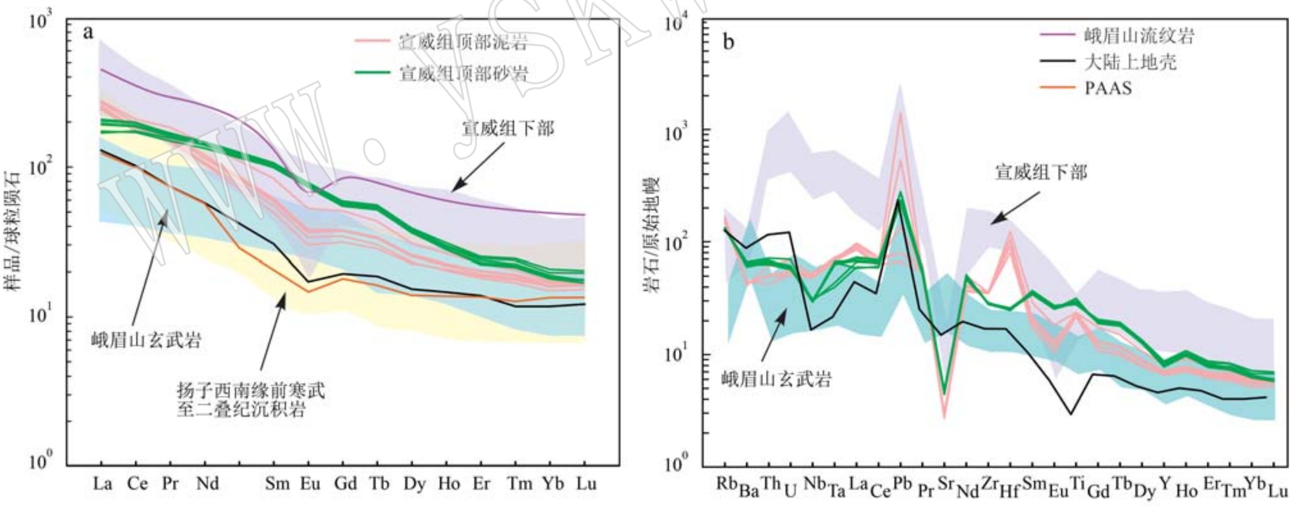

图 5 峨眉山地区宣威组顶部泥岩、砂岩稀土元素球粒陨石标准化配分模式图(a)和微量元素原始地幔标准化蛛网图(b)（原始地幔标准、球粒陨石标准据 Sun 和 McDonough, 1989）

Fig. 5 Chondrite-normalized REE patterns (a) and primitive mantle-normalized trace element spidergrams (b) of mudstone and sandstone samples at the top of the Xuanwei Formation in the Emeishan area (primitive mantle and chondrite form Sun and McDonough, 1989)

数据来源：平均后太古代页岩(PAAS)据 Taylor 和 McLennan(1985)；大陆上地壳(UCC)据 Rudnick 和 Gao(2003)；宣威组下部引自 He 等(2007)、Zhang 等(2010)、Zhao 等(2016)；峨眉山玄武岩、峨眉山流纹岩引自 Xu 等(2001)、Xiao 等(2004)、Fan 等(2008)、Zi 等(2012)、Zhu 等(2017)

data sources: mean post Archean shale (PAAS) form Taylor and McLennan, 1985; upper continental crust (UCC) form Rudnick and Gao, 2003; the lower part of Xuanwei Formation from He *et al.*, 2007; Zhang *et al.*, 2010; Zhao *et al.*, 2016; Emeishan basalt and rhyolite from Xu *et al.*, 2001; Xiao *et al.*, 2004; Fan *et al.*, 2008; Zi *et al.*, 2012; Zhu *et al.*, 2017

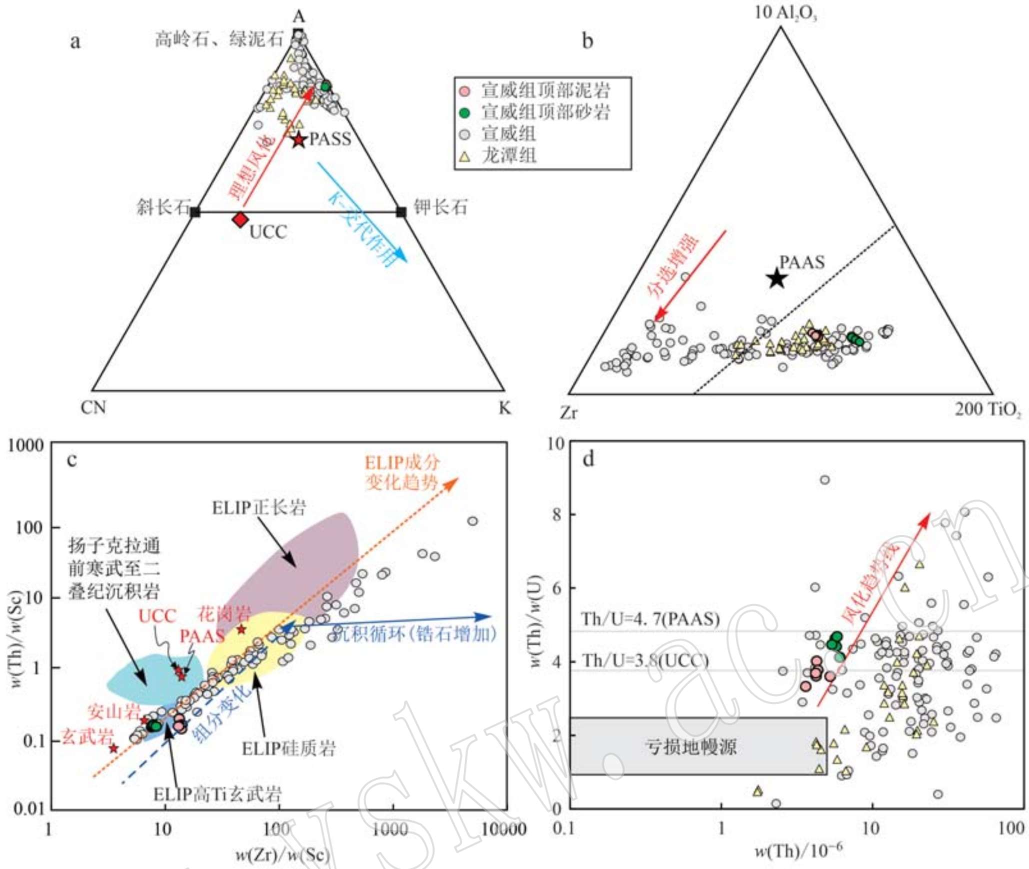

图 6　峨眉山地区宣威组顶部泥岩、砂岩的 A-CN-K(a, Nesbitt and Young, 1984)、Al_2O_3-Zr-TiO_2(b, Garcia *et al.*, 1991)、Th/Sc-Zr/Sc (c, McLennan *et al.*, 1993)和 Th/U-Th(d, McLennan *et al.*, 1993)判别图解

Fig. 6　A-CN-K(a, after Nesbitt and Young, 1984), Al_2O_3-Zr-TiO_2(b, after Garcia *et al.*, 1991), Th/Sc-Zr/Sc(c, after McLennan *et al.*, 1993) and Th/U-Th (d, after McLennan *et al.*, 1993) discrimination diagrams of mudstone and sandstone at the top of the Xuanwei Formation in Emeishan area

原始地幔、球粒陨石标准据 Sun 和 McDonough (1989)；平均后太古代页岩(PAAS)据 Taylor 和 McLennan (1985)；大陆上地壳(UCC)据 Rudnick 和 Gao (2003)；宣威组引自 He 等(2007)、Zhang 等(2010)、Zhao 等(2016)；龙潭组引自 He 等(2020)、于鑫等 (2017)；峨眉山高 Ti 玄武岩、峨眉山流纹岩、峨眉山硅质岩、峨眉山正长岩引自 Xu 等(2001)、Xiao 等(2004)、Fan 等(2008)、Zi 等(2012)、Zhu 等(2017)；扬子克拉通前寒武系至二叠系沉积岩引自 Li 等(2003)、肖加飞(2005)、Sun 等(2008)、Zhao 和 Zhou (2008)、杜利林等 (2013)、Wang 等(2014)

primitive mantle and chondrite form Sun and McDonough, 1989; mean post Archean shale(PAAS) from Taylor and McLennan, 1985; upper continental crust(UCC) form Rudnick and Gao, 2003; Xuanwei Formation from He *et al.*, 2007; Zhang *et al.*, 2010; Zhao *et al.*, 2016; Longtan Formation from Yu Xin *et al.*, 2017 and He *et al.*, 2020; Emeishan high-Ti basalt, Emeishan rhyolite, Emeishan silicalite and Emeishan syenite from Xu *et al.*, 2001; Xiao *et al.*, 2004; Fan *et al.*, 2008; Zi *et al.*, 2012; Zhu *et al.*, 2017; Precambrian to Permian sedimentary rock of Yangtze Craton from Li *et al.*, 2003; Xiao Jiafei, 2005; Sun *et al.*, 2008; Zhao and Zhou, 2008; Du Lilin *et al.*, 2013; Wang *et al.*, 2014

风化强度呈正相关,不同的源区和风化强度对应不同的比值(McLennan and Taylor, 1980; McLennan *et al.*, 1993)。宣威组沉积岩具有高的 Th/U 值(3.30～4.69; 平均值为 4.09),这表明存在氧化条件(UCC>3.8, Taylor and McLennan, 1985)。在用来评价连续的化学风化作用和沉积再循环过程的 Th-Th/U 双变量图上,大多数样品沿着风化趋势绘制(图 6d),表明峨眉山地区处于源区的边缘,经历了强烈的构造隆起,并经历了快速剥蚀和沉积。

4.2　物源分析

扬子克拉通西缘二叠系沉积岩沉积于扬子克拉通之上,紧邻峨眉山大火成岩省,因此扬子克拉通及峨眉山大火成岩省是物源的可能来源(图 1,Zhou *et al.*, 2013)。考虑到峨眉山大火成岩省的火山序列主要由底部的低 Ti 玄武岩、上部的高 Ti 玄武岩和顶部的酸性火山岩组成,而在东部则主要为高 Ti 玄武岩(Xu *et al.*, 2001; Xiao *et al.*, 2004),结合宣威组样品中大量的火山碎屑(图 3)及扬子克拉通西缘晚

二叠世沉积岩近源堆积的特征,指示峨眉山大火成岩省的东部区域可能是其物源区之一。但前人对扬子克拉通西缘晚二叠世沉积岩的研究,认为扬子克拉通西南缘为宣威组提供了部分碎屑物源(Xu *et al.*, 2001; Ali *et al.*, 2005; Zhou *et al.*, 2013; 何冰辉, 2015; 何冰辉等, 2017)。

全岩地球化学数据蕴含了沉积物源的重要信息(Roser and Korsch, 1986; Cullers, 2000)。在稀土元素球粒陨石标准化配分模式图及微量元素原始地幔标准化蛛网图中,上二叠统沉积岩具有相同的特征,并与峨眉山高 Ti 玄武岩相似(图 5),这表明峨眉山高 Ti 玄武岩可能为上二叠统提供了部分物源。在 Ni-V-Th 三元图上,大部分晚二叠世沉积岩接近 V-Ni 线,少部分靠近长英质源区,反映了其具铁镁质岩石和长英质岩石的混合物源特征(图 7a)。此外,晚二叠世沉积岩在 Co/Th-La/Sc 图中具有高的 Co/Th 值和低的 La/Sc 值(图 7b),在 Th/Sc-Zr/Sc 图中具有低的 Th/Sc 值和较低的 Zr/Sc 值(图 6c),意味着化学成熟度低,沉积循环弱,沉积岩主要受物质组分的改变控制。另外,在微量元素双变量图解中大部分的二叠系沉积岩都靠近峨眉山高 Ti 玄武岩范围(图 7b、7c),少量二叠系沉积岩位于扬子克拉通前寒武系到二叠系沉积岩范围(图 7b)。

在风化、运输和成岩过程中一些元素通常被认为是非活动性元素,如 Ti(Nesbitt and Markovics, 1997)和 Al(Ji *et al.*, 2000; Das and Krishnaswami, 2007)。宣威组沉积岩经历了强烈的化学风化作用和弱的分选作用(图6),因此,Al_2O_3/TiO_2值的变化

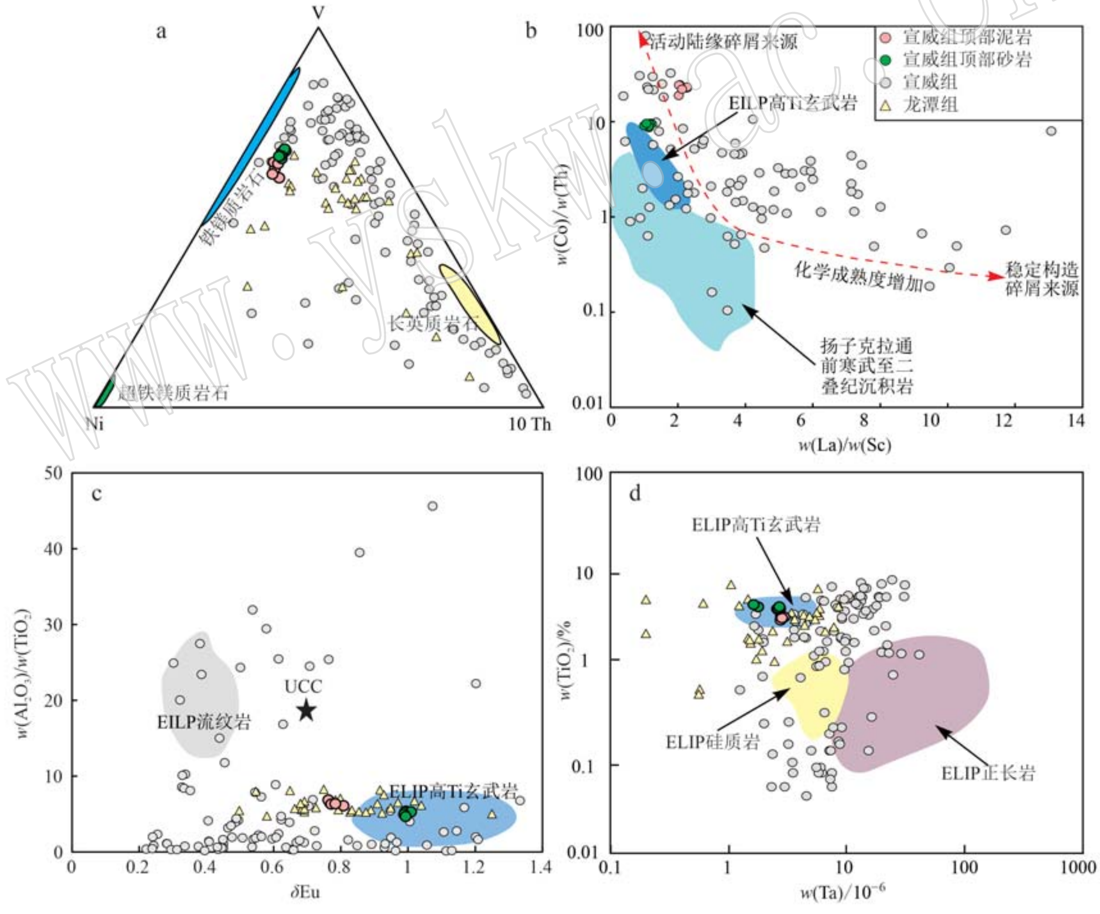

图 7 峨眉山地区宣威组沉积岩的 V-Ni-Th(a, 底图据 Bracciali *et al.*, 2007)、Co/Th-La/Sc(b, 底图据 McLennan *et al.*, 1993; Zhao *et al.*, 2017)、Al_2O_3/TiO_2-δEu(c, 底图据 Zhao *et al.*, 2017)和 TiO_2-Ta(d, 底图据 Zhao *et al.*, 2017)物源判别图解(数据来源同图 6)

Fig. 7 V-Ni-Th (a, after Bracciali *et al.*, 2007), Co/Th-La/Sc (b, after McLennan *et al.*, 1993; Zhao *et al.*, 2017), Al_2O_3/TiO_2-δEu (c, after Zhao *et al.*, 2017) and TiO_2-Ta (d, after Zhao *et al.*, 2017) provenance discrimination diagrams of Xuanwei Formation sediments in Emeishan area (the data sources are shown in Fig. 6)

是由于沉积岩中镁铁质组分的加入造成的(Willis *et al.*, 1988)。来自宣威组的泥岩、砂岩样品具有较低的 Al_2O_3/TiO_2 值,类似于峨眉山高 Ti 玄武岩(2.7~8.1; Zhu *et al.*, 2018),低于峨眉山流纹岩(>10.0; Zhu *et al.*, 2018)。宣威组泥岩、砂岩落入或靠近峨眉山高 Ti 玄武岩区域附近(图 6a),支持了宣威组物源有峨眉山高 Ti 玄武岩的来源。另外,扬子克拉通西缘的晚二叠世沉积岩(宣威组、龙潭组等)具有变化的 Al_2O_3/TiO_2、Th/U、La/Sc、Th/Sc、δEu 和 Co/Th 值(图 6、图 7),并表现出弱的 Eu 负异常和类似于 UCC 的球粒陨石标准化稀土元素配分模式(图 4)。扬子克拉通西缘上二叠统的沉积岩大部分位于靠近峨眉山高 Ti 玄武岩范围,少部分位于或靠近扬子克拉通前寒武至二叠系沉积岩范围(图 6c、图 7b)。

综上所述,地球化学特征和判别图解都表明晚二叠世扬子克拉通西南缘的沉积岩不仅从峨眉山大火成岩省东部区域接收了大量的高 Ti 玄武岩碎屑,还从扬子克拉通得到了物源补给。

4.3　沉积古环境

沉积岩中的元素含量、元素组合及相关比值可以为古环境的特征提供可靠信息(Rimmer *et al.*, 2004; Algeo and Maynard, 2004; 张天福等, 2016; 高莲凤等, 2017; 谭聪等, 2019)。宣威组顶部泥岩的 Sr/Ba 值(0.19~0.21)及 V/Ni 值(2.08~2.89)符合陆相泥岩的特征,指示古沉积环境为淡水沉积环境。这与前人对宣威组沉积环境与沉积相的认识相符(李明龙等, 2014; Bercovici *et al.*, 2015; 张天福等, 2016; 田景春等, 2016; 张廷山等, 2017)。但宣威组泥岩和砂岩中观察到的海绿石似乎表明峨眉山地区此时是海洋沉积环境(图 3c、3d)(Odin and Matter, 1981; 梅冥相等, 2008)。Lweis(1964)认为海绿石能够通过短距离再搬运作用而离开其形成地点,但还是保存在同时代的沉积地层中(梅冥相等, 2008; 陈淑慧等, 2014)。Fischer(1990)认为地层中的海绿石也可以是从更老的地层中受外力搬运而来再沉积的海绿石颗粒。潘江涛等(2022)在永善宣威组下部中发现了海绿石,马玉孝等(2002)在攀枝花地区的上震旦统把关河组剖面中发现了 6 层含海绿石砂岩,钱逸等(1984)云南晋宁梅树村震旦系-寒武系中发现了海绿石,这些发现表明宣威组及更老的地层中拥有丰富的海绿石,结合宣威组顶部泥岩及砂岩的物源,我们认为宣威组顶部的海绿石可能是在宣威组及更老地层中的海绿石通过搬运再次沉积的。

一般认为泥岩中 U/Th 值大于 0.75 且 δU 大于 1,为缺氧环境;U/Th 值小于 0.75 且 δU 小于 1 为富氧环境(Jones and Manning, 1994; 吴朝东等, 1999; 张天福等, 2016)。宣威组顶部泥岩的 U/Th 值为 0.21~0.30,平均为 0.25;δU 为 0.78~0.95,平均为 0.85,指示为富氧环境。另外,宣威组顶部泥岩中 V/Cr 值(1.87~1.96,平均 1.93)及 Ni/Co 值(1.29~1.42,平均 1.35)也符合沉积时水体环境为富氧的特征(Jones and Manning, 1994; 张天福等, 2016)。此外,宣威组顶部泥岩的 Ce_{anom} 值(-0.06~-0.05; 李明龙等, 2014),Eu 负异常(δEu=0.33~0.61; 田景春等, 2016)也表明为氧化环境。同时,宣威组顶部砂岩样品的 Fe^{2+}/Fe^{3+} 范围在 0.23~0.30,平均为 0.26,指示砂岩沉积时为氧化环境(熊小辉等, 2011)。

Zhang 等(2010)在对贵州西部的宣威组研究中,认为宣威组碳质页岩的沉积环境为海水参与的缺氧环境,并且有热液作用,而砂质页岩形成于缺氧到富氧的过渡环境。阙薇(2008)对扬子克拉通西缘不同地区的二叠-三叠系界线附近采集的黏土岩进行了元素地球化学测试与分析,发现江油和广元地区的二叠纪末期海相沉积环境也为富氧环境。张廷山等(2017)发现筠连地区上二叠统宣威组广泛发育曲流河相、潮坪相和少量混积台地相沉积,煤层主要发育于潮上带沼泽微相带中。邓江红(2013)认为峨眉山宣威组中的斜层理、冲刷面等构造,表明宣威组沉积相为沼泽相-河流沼泽相。另外,宣威组的特征为由西向东地层厚度逐渐增大,并且沉积岩层自西向东由河流相变为潮坪相再往东变为碳酸盐岩台地相,这种古地理条件与沉积相分布特征(张廷山等, 2017),说明峨眉山地区在二叠纪经历了海陆变迁。因此,我们认为峨眉山宣威组为海陆过渡相沉积,峨眉山二叠纪晚期已经进入海退阶段,沉积古环境也变为富氧的淡水沉积环境。

4.4　沉积构造背景

沉积岩的全岩地球化学已被用于区分沉积盆地的构造环境(Bhatia, 1983; Bhatia and Crook, 1986; Roser and Korsch, 1986)。稀土元素常被用于区分主动和被动边缘构造环境(Bhatia, 1985; McLennan *et al.*, 1993; Verma and Armstrong-Altrin, 2013)。根据 Bhatia(1985)的研究,被动边缘的稀土元素分布特征类似于 UCC 和后太古代澳大利亚页岩

(PAAS)的平均值(Taylor and McLennan, 1985),具有相对明显的 Eu 负异常。宣威组沉积岩的稀土元素特征与 Eu 异常不同于平均上地壳和后太古代澳大利亚页岩(图 5),表明其沉积环境并非是被动大陆边缘。而沉积岩中某些不活动元素的含量及其比值能够进一步判别并划分沉积构造环境(如大洋岛弧、大陆边缘弧、活动大陆边缘、被动大陆边缘)(Bhatia, 1983; Bhatia and Crook, 1986; McLennan and Taylor, 1991)。宣威组顶部沉积岩的 LREE/HREE 值接近活动大陆边缘砂岩,且相关的微量元素比值(如 La/Y)也与活动大陆边缘砂岩相似(表 3)。实际上,微量元素判别图解也给出一致的结果,上二叠统宣威组沉积岩落在全球活动大陆边缘砂岩范围,暗示它们是在活动大陆边缘环境下沉积的(图 8b~8d)。另外,宣威组顶部泥岩和砂岩较低的 K_2O (2.98%~3.30%)及 Na_2O (0.01%~0.11%)含量(图 6a),暗示其可能经历了短距离运输和快速堆积,物源来自于地壳抬升地区。

表 3 宣威组泥岩、砂岩与其他构造背景砂岩的地球化学参数对比

Table 3 Comparation of geochemical parameters between the mudstone and sandstone from Xuanwei Formation and sandstone of different tectonic settings

构造环境	宣威组平均	宣威组泥岩平均	宣威组砂岩平均	大洋岛弧	大陆边缘弧	活动大陆边缘	被动大陆边缘
La	53.61	62.87	45.72	8±1.7	27±4.5	37	39
Ce	115.85	116.67	114.80	19±3.7	59±8.2	78	85
ΣREE	712.43	982.77	257.18	58±10	146±20	186	210
LREE/HREE	8.20	9.58	6.48	3.8±0.9	7.7±1.7	9.1	8.5
La/Yb	18.28	22.86	14.25	4.2±1.3	11.0±3.6	12.5	15.9
$(La/Yb)_N$	10.31	11.16	8.59	2.8±0.9	7.5±2.5	8.5	10.5
δEu	0.90	0.57	1.19	1.04±0.11	0.79±0.13	0.6	0.56
Rb/Sr	1.25	1.70	0.86	0.05±0.05	0.65±0.33	0.89±0.24	1.19±0.40
Zr/Th	74.57	93.78	56.24	48.0±13.4	21.5±2.4	9.5±0.7	19.1±5.8
La/Sc	1.60	2.13	1.13	0.55±0.22	1.82±0.3	4.55±0.8	6.25±1.4
La/Y	1.58	1.96	1.24	0.48±0.12	1.02±0.07	1.33±0.09	1.31±0.26
La/Th	11.20	14.74	8.06	4.26±1.20	2.36±0.30	1.77±1.1	2.20±0.47
Zr/Hf	27.92	13.30	40.99	46	36	26	30

注:表中元素含量单位为 10^{-6};大洋岛弧、大陆边缘弧、活动大陆边缘和被动大陆边缘数据据 Bhatia 和 Crook(1986)。

中二叠世末期,金沙江-哀牢山洋由南向北俯冲导致弧后发生大规模伸展,峨眉裂谷活动,进一步的地壳隆升导致茅口组受到不同程度的剥蚀(梅庆华等, 2014)。随后,峨眉地幔柱开始活动并引发大规模火山喷发(260.55~257.22 Ma)形成了峨眉山大火成岩省(Zhong *et al.*, 2014; Li *et al.*, 2018; Huang *et al.*, 2022),使得四川盆地周缘中二叠世末期的气候变暖,这可能大大加强了该地区的化学风化作用(Huang *et al.*, 2022)。晚二叠世期间,峨眉地幔柱的活动使得位于扬子克拉通西南边缘的康滇裂谷带重新开始活跃,并在峨眉山地区发育一套大陆裂谷边缘玄武岩(熊舜华等, 1984)。由于康滇裂谷带的活动,扬子克拉通西南缘进入隆升剥蚀阶段,西南地区整体进入海退时期,呈现出西高东低的古地理格局(图 9b)(邵龙义等, 2013; 高彩霞, 2015; Huang *et al.*, 2021)。宣威组沉积岩的构造判别图解也支持晚二叠世扬子克拉通西南缘是一个活动大陆边缘环境(图 8)。基于上述讨论,我们认为在晚二叠世,峨眉山地区的沉积岩主要受物质组分的变化控制,除接受了峨眉山大火成岩省中高 Ti 玄武岩提供的碎屑物源,还接受了扬子克拉通的物源补给,其沉积构造背景为扬子克拉通西缘的活动大陆边缘环境(图 9c)。

5 结论

(1) 峨眉山宣威组沉积岩中大量的高岭石、高的 CIA 值、高的 PIA 值及低的 ICV 值表明源区遭受了强烈的化学风化作用,并经历了快速剥蚀和沉积。

(2) 峨眉山宣威组沉积岩的微量元素含量与大陆上地壳(UCC)相比,相对富集高场强元素,相对亏损大离子亲石元素,结合沉积岩判别图解,认为宣威组沉积岩的物源属于混合物源,物源不仅来自于峨眉山高 Ti 玄武岩,还接受了扬子克拉通的物源补给。

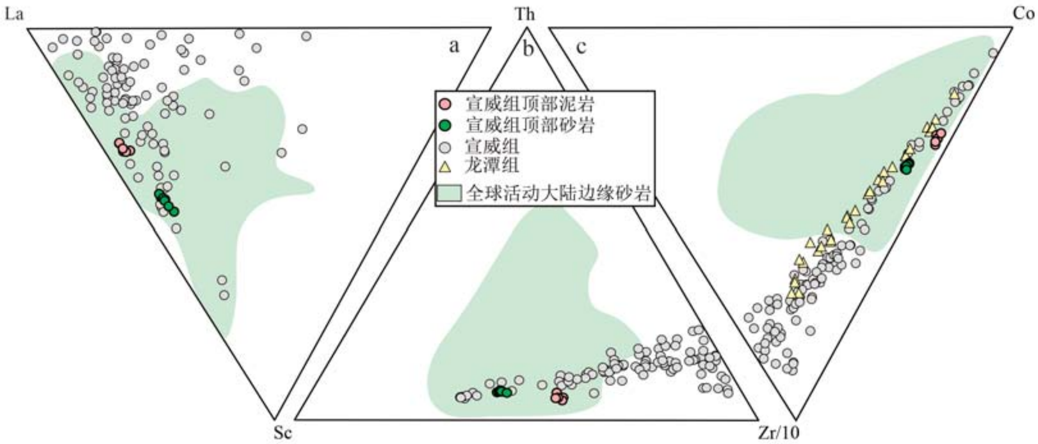

图 8　峨眉山地区宣威组沉积岩的 La-Th-Sc(a)、Th-Sc-Zr/10(b)和 Th-Co-Zr/10(c)构造判别图(Bhatia and Crook, 1986)

Fig. 8　La-Th-Sc(a), Th-Sc-Zr(b) and Th-Co-Zr(c) tectonic discrimination maps of sediments from Xuanwei Formation in Emeishan area (after Bhatia and Crook, 1986)

全球活动大陆边缘砂岩据 Verma 和 Armstrong-Altrin (2016),其他数据来源同图 6

the global scope of active continental margin sandstones from Verma and Armstrong-Altrin, 2016, the other data sources are shown in Fig. 6

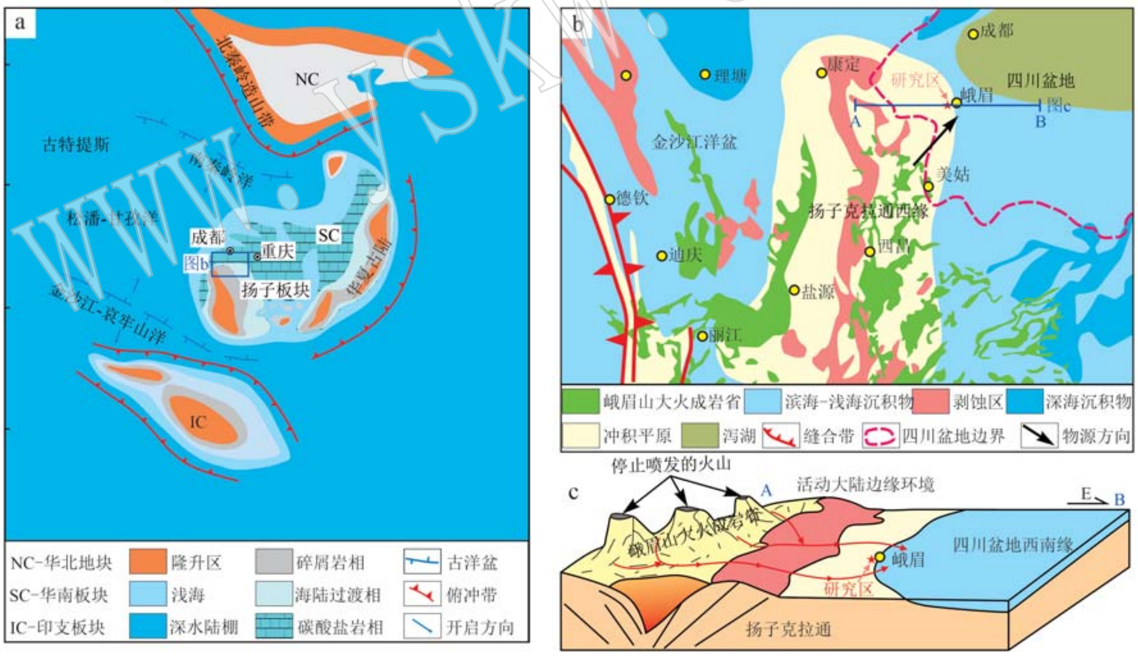

图 9　晚二叠世华南板块与相邻板块海陆分布和主要沉积相重建图[a, 据 Cocks 和 Torsvik(2013)、Zhao 等(2018)、邓煜霖等(2018)和 Huang 等(2021)修改]、晚二叠世扬子克拉通周缘构造沉积盆地模型[b, 据马永生(2009)和 Zhu 等(2018)修改,峨眉山大火成岩省位置据 Li 等 (2021)]和晚二叠世扬子克拉通西南缘地区古地理演化模式图[c, 据 Yin 和 Harrison (2000)、Zhu 等(2018)修改]

Fig. 9　Reconstruction of the sea-land distribution and main sedimentary facies of South China plate and adjacent plates in Late Permian (a, modified from Cocks and Torsvik, 2013; Zhao *et al.*, 2018; Deng Yulin *et al.*, 2018; Huang *et al.*, 2021), model of tectonic sedimentary basin around the Yangtze Craton in Late Permian (b, modified from Ma Yongsheng, 2009; Zhu *et al.*, 2018, ELIP location from Li *et al.*, 2021), paleogeographic evolution model of the southwestern Yangtze Craton in Late Permian (c, modified from Yin and Harrison, 2000; Zhu *et al.*, 2018)

(3) 根据峨眉山宣威组全岩地球化学特征,结合前人对宣威组沉积相的研究,认为峨眉山二叠纪晚期已经进入海退阶段,沉积古环境也变为富氧的淡水沉积环境。

(4) 峨眉山宣威组的 LREE/HREE 及 La/Y 值接近活动大陆边缘砂岩,微量元素判别图解也表明其是在活动大陆边缘环境下沉积的,因此认为扬子克拉通西缘峨眉山地区晚二叠世期间处于活动大陆边缘沉积环境。

References

Algeo T J and Maynard J B. 2004. Trace-element behavior and redox facies in core shales of Upper Pennsylvanian Kansas-type cyclothems[J]. Chemical Geology, 206(3~4): 289~318.

Ali J R, Thompson G M, Zhou M F, *et al*. 2005. Emeishan large igneous province, SW China[J]. Lithos, 79: 475~489.

Bercovici A, Ying Cui, Marie-Béatrice Forel, *et al*. 2015. Terrestrial paleoenvironment characterization across the Permian-Triassic boundary in South China[J]. Journal of Asian Earth Sciences, 98: 225~246.

Bhatia M R. 1983. Plate tectonics and geochemical composition of sandstones[J]. The Journal of Geology, 91(6): 611~627.

Bhatia M R. 1985. Rare earth element geochemistry of Australian Paleozoic graywackes and mudrocks: Provenance and tectonic control[J]. Sedimentary Geology, 45(1~2): 97~113.

Bhatia M R and Crook K A W. 1986. Trace element characteristics of greywackes and tectonic discrimination of sedimentary basins[J]. Contributions to Mineralogy and Petrology, 92(2): 181~193.

Bracciali L, Marroni M, Pandolfi L, *et al*. 2007. Geochemistry and petrography of western Tethys Cretaceous sedimentary covers (Corsica and Northern Apennines): From source areas to configuration of margins[J]. Special Papers-Geological Society of America, 420: 73.

Chen Bin, Li Yong, Wang Weiming, *et al*. 2016. The provenance and tectonic setting of Late Triassic Xujiahe Formation in the Longmenshan foreland basin, SW China[J]. Acta Geologica Sinica, 90(5): 857~872(in Chinese with English abstract).

Chen Fenglin, Xie Yuan, Cui Xiaozhuang, *et al*. 2018. Geochronology, geochemistry and tectonic implications of basalts from the Ebian Group in the western Yangtze Block, South China[J]. Journal of Mineralogy and Petrology, 38(3): 76~86(in Chinese with English abstract).

Chen J F and Jahn B M. 1998. Crustal evolution of southeastern China: Nd and Sr isotopic evidence[J]. Tectonophysics, 284: 101~133.

Chen Jianping, Li Wei, Ni Yunyan, *et al*. 2018. The Permian source rocks in the Sichuan Basin and its natural gas exploration potential (Part 1): Spatial distribution of source rocks[J]. Nat. Gas. Ind., 38(5): 1~16(in Chinese with English abstract).

Chen Lu. 2014. Study of the Relic Assemblage of the Upper Cretaceous Jiaguan Formation in the Emei area, Sichuan [D]. Chengdu: Southwest Petroleum University(in Chinese with English abstract).

Chen Shuhui, Li Yun, Hu Zuowei, *et al*. 2014. Genesis, diagnostic role and age significance of glauconites[J]. Acta Petrologica et Mineralogica, 33(5): 971~979 (in Chinese with English abstract).

Chen W, Liu J, Wang Z, *et al*. 2003. Study on lithofacies palaeogeography during the Permian Emeishan basalt explosion in Guizhou Province[J]. Journal of Palaeogeography, 5(1): 17~28.

Chen Zongqing. 2011. Exploration for shale gas of Longtan member in Permian Leping formation, Sichuan Basin[J]. Natural Gas Technology and Economy, 5(2): 21~26, 78(in Chinese with English abstract).

Chung S L and Jahn B M. 1995. Plume-lithosphere interaction in generation of the Emeishan flood basalts at the Permian-Triassic boundary [J]. Geology, 23(10): 889~892.

Cocks L R M and Torsvik T H. 2013. The dynamic evolution of the Palaeozoic geography of eastern Asia[J]. Earth Sci. Rev., 117: 40~79.

Courtillot V, Jaupart C, Manighetti I, *et al*. 1999. On causal links between flood basalts and continental breakup[J]. Earth and Planetary Science Letters, 166(3): 177~195.

Cox R, Lowe D R and Cullers R L. 1995. The influence of sediment recycling and basement composition on evolution of mudrock chemistry in the southwestern United States[J]. Geochimica et Cosmochimica Acta, 59(14): 2 919~2 940.

Cullers R L. 2000. The geochemistry of shales, siltstones and sandstones of Pennsylvanian-Permian age, Colorado, USA: Implications for provenance and meta morphic studies[J]. Lithos, 51: 181~203.

Das A and Krishnaswami S. 2007. Elemental geochemistry of river sediments from the Deccan Traps, India: Implications to sources of elements and their mobility during basalt-water interaction[J]. Chemical Geology, 242(1~2): 232~254.

Deng Jianghong. 2013. Tutorial on Geological Awareness Practice in Emei Mountain[M]. Beijing: Geological Publishing House(in Chinese with English abstract).

Deng Xusheng. 2019. Analysis of Upper Permian Sedimentary Phases and Sediment Sources in the Northern Margin of the Right River Basin

[D]. China University of Geosciences (in Chinese with English abstract).

Deng Yulin, Lang Xinghai, Cui Zhiwei, *et al*. 2018. A study of the claystone around the Permian-Trassic boundary along the Cilinbao section at Majiaoba, Jiangyou, Sichuan Province[J]. Acta Petrologica et Mineralogica, 37(3): 417~433 (in Chinese with English abstract).

Dong J, Guo Q W, Zhu X C, *et al*. 2006. Longmen shan fold-thurst belt and its relation to the western Sichuan Basin in central China: New insights from hydrocarbon exploration[J]. The American Association of Petroleum Geologists, 90(9): 1 425~1 447.

Du Lilin, Guo Jinghui, Geng Yuansheng, *et al*. 2013. Age and tectonic setting of the Yanbian Group in the southwestern Yangtze Block: Constraints from clastic sedimentary rocks[J]. Acta Petrologica Sinica, 29(2): 641~672 (in Chinese with English abstract).

Enkelmann E, Weislogel A, Ratschbacher L, *et al*. 2007. How was the Triassic Songpan-Ganzi basin filled? A provenance study[J]. Tectonics, 26(4): 640~641.

Fan W M, Wang Y J, Peng T P, *et al*. 2008. Ar-Ar and U-Pb geochronology of Late Paleozoic basalts in western Guangxi and its constraints on the eruption age of Emeishan basalt magmatism[J]. Chinese Science Bulletin, 21(49): 2 318~2 327.

Fedo C M, Nesbitt H W and Young G M. 1995. Unraveling the effects of potassium metaso matism in sedimentary rocks and paleosols, with implications for paleoweathering conditions and provenance[J]. Geology, 23: 921~924.

Feng Chong, Zou Huayao, Guo Tonglou. 2015. Late Permian-Early Triassic sedimentary evolution in Sichuan Basin and its significance on gas accumulation[J]. Journal of Earth Sciences and Environment, 37(4): 44~53(in Chinese with English abstract).

Fischer H. 1990. Glauconite formation: Discussion of the terms authigenic, perigenic, allogenic, and meta-allogenic[J]. Eclogae Geologicae Helvetiae, 83(1): 1~6.

Gao Caixia. 2015. Study on Late Permian Stratigraphy-paleogeography and Coal Aggregation Patterns in Sichuan, Chongqing, Yunnan and Guizhou[D]. China University of Mining and Technology(Beijing) (in Chinese with English abstract).

Gao Lianfeng, Zhou Wei, Zhang Ying, *et al*. 2017. Geochemical characteristics of marine strata and the evolution of paleoceanographic environment from Late Jurassic to Early Cretaceous in Gonggar, Southern Tibet[J]. Earth Sci. Front., 24(1): 195~204(in Chinese with English abstract).

Garcia D, Coelho J and Perrin M. 1991. Fractionation between TiO_2 and Zr as a measure of sorting within shale and sandstone series (northern Portugal)[J]. European Journal of Mineralogy, 3: 401~414.

Geng Yuansheng, Kuang Hongwei, Liu Yongqing, *et al*. 2017. Subdivision and correlation of the Mesoproterozoic stratigraphy in the western and northern margins of Yangtze Block[J]. Acta Geologica Sinica, 91(10): 2 151~2 174 (in Chinese with English abstract).

He B, Xu Y G, Huang X L, *et al*. 2007. Age and duration of the Emeishan flood volcanism, SW China: Geochemistry and SHRIMP zircon U-Pb dating of silicic ignimbrites, post-volcanic Xuanwei Formation and clay tuff at the Chaotian section[J]. Earth and Planetary Science Letters, 255(3~4): 306~323.

He B, Xu Y G, Wang Y M, *et al*. 2005. The magnitude of crustal uplift prior to the eruption of the Emeishan basalt: Inferred from sedimentary records[J]. Geotectonica et Metallogenia, 29(3): 316~320.

He B, Xu Y, Xiao L, *et al*. 2003. Generation and spatial distribution of the Emeishan large igneous province: New evidence from stratigraphic records[J]. Acta Geologica Sinica, 77(2): 194~202.

He Binghui. 2015. Stratigraphic Record of the Upper Permian Xuanwei Formation in the Tectonic Activity of the Emei Mountain Large Igneous Province[D]. China University of Geosciences (Beijing) (in Chinese with English abstract).

He Binghui, Liu Shaofeng and Wu Peng. 2017. LA-ICP-MS U-Pb geochronology and its geological implications of the detrital zircons from the lower strata of Upper Permian Xuanwei formation in Zhehai town, eastern Yunnan Province[J]. Geological Survey and Research, (2): 126~133, 146 (in Chinese with English abstract).

He Q, Dong T, He S, *et al*. 2020. Sedimentological and geochemical characterization of the Upper Permian transitional facies of the Longtan Formation, northern Guizhou Province, southwest China: Insights into paleo-environmental conditions and organic matter accumulation mechanisms[J]. Marine and Petroleum Geology, 118: 104446.

Hu Ruizhong, Tao Yan, Zhong Hong, *et al*. 2005. Mineralizaiton system of a mantle plume: A case study from the Emeishan igneous province, southwest China[J]. Earth Science Frontiers, 12(1): 42~54 (in Chinese with English abstract).

Huang Dan. 2012. Stratigraphy of the Upper Permian Changxing Formation-Lower Triassic Feixianguan Formation in the Western Sichuan Basin[D]. Jingzhou: Changjiang University (in Chinese with English abstract).

Huang H Y, He D F, Li Y Q, *et al*. 2021. Late Permian tectono-sedimentary setting and basin evolution in the Upper Yangtze region, South China: Implications for the formation mechanism of intra-platform depressions —Science Direct[J]. Journal of Asian Earth Sciences, 205: 104599.

Huang H, Huyskens M, Yin Q, *et al*. 2022. Eruptive tempo of Emeishan large igneous province, southwestern China and northern Vietnam: Relations to biotic crises and paleoclimate changes around the Guadalupian-Lopingian boundary[J/OL]. Geology, https://doi.org/10.1130/G50183.1.

Ivanova V V, Nikol'skii P A, Tesakov A S, *et al*. 2015. Geochemical indicators of paleoclimatic changes in the Cenozoic deposits of the Lower Aldan Basin[J]. Geochemistry International, 53: 358~368.

Ji H, Ouyang Z, Wang S, *et al*. 2000. Element geochemistry of weathering profile of dolomitite and its implications for the average chemical composition of the upper-continental crust[J]. Science in China Series D: Earth Sciences, 43(1): 23~35.

Jiang Xiaoli, Gong Daxing, Zhou Jiayun, *et al*. 2022. The research progress and problems of rare earth elements of rare earth rich clay rock Permian Xuanwei Formation in the Yunnan-Guizhou border region [J]. Multipurpose Utilization of Mineral Resources, (1): 32~41(in Chinese with English abstract).

Jiao Xin, Liu Yiqun, Yang Wan, *et al*. 2017. Progress on sedimentation of subaqueous volcanic eruption[J]. Advances in Earth Science, 32(9): 926~936 (in Chinese with English abstract).

Jones B and Manning D A. 1994. Comparison of geochemical indices used for the interpretation of palaeoredox conditions in ancient mudstones [J]. Chemical Geology, 111(1~4): 111~129.

Lai Xulong, Sun Yadong and Jiang Haishui. 2009. The relationship between volcanism of Emeishan large igneous province and mass extinction during middle-late Permian transition[J]. Bulletin of National Natural Science Foundation of China, 6: 353~356(in Chinese with English abstract).

Lewis D W. 1964. 'Perigenic': A new term[J]. Journal of Sedimentary Research, 34(4): 875~876.

Li Chen, Lang Xinghai, Deng Yulin, *et al*. 2020. Geochronological and geochemical characteristics of the claystone (mung bean rock) at the bottom of the Leikoupo Formation in the Emeishan area, Sichuan Basin, China[J]. Bulletin of Mineralogy, Petrology and Geochemistry, 39(4): 810~825(in Chinese with English abstract).

Li Minglong, Zheng Deshun, Dai Guangzhong, *et al*. 2014. Geochemical characteristics of the Jurassic argillaceous rocks of the Jiyuan Basin, Western Henan and the implications for environments and provenances [J]. Acta Geologica Sinica, 88(2): 228~238(in Chinese with English abstract).

Li W, Shi Z, Yin G, *et al*. 2021. Origin and tectonic implications of the early Middle Triassic tuffs in the western Yangtze Craton: Insight into whole-rock geochemical and zircon U-Pb and Hf isotopic signatures [J]. Gondwana Research, 93: 142~161.

Li Y, He H, Ivanov A, *et al*. 2018. $^{40}Ar/^{39}Ar$ age of the onset of high-Ti phase of the Emeishan volcanism strengthens the link with the end-Guadalupian mass extinction[J]. International Geology Review, 60: 1 906~1 917.

Li Z X, Li X H, Kinny P D, *et al*. 2003. Geochronology of Neoproterozoic syn-rift magmatism in the Yangtze Craton, South China and correlations with other continents: Evidence for a mantle superplume that broke up Rodinia[J]. Precambrian Research, 122(1~4): 85~109.

Liang Digang, Guo Tonglou, Bian Lizeng, *et al*. 2009. Some progresses on studies of hydrocarbon generation and accumulation in marine sedimentary regions, Southern China (Part 3): Controlling factors on the sedimentary facies and development of Palaeozoic marine source rocks [J]. Marine Origin Petroleum Geology, (2): 1~19 (in Chinese with English abstract).

Liang Xinquan, Zhou Yun, Jiang Ying, *et al*. 2013. Difference of sedimentary response to Dongwu movement: Study on LA-ICP-MS U-Pb ages of detrital zircons from Upper Permian Wujiaping or Longtan Formation from the Yangtze and Cathaysia blocks[J]. Acta Petrologica Sinica, 29(10): 3 592~3 606(in Chinese with English abstract).

Lin Maobing. 1994. Discussion on the basic textural style of the nappe tectonic belt in Longmen Mountains[J]. Journal of Chengdu College of Geology, 21(3): 1~7 (in Chinese with English abstract).

Liu Hefu, Liang Huishe, Cai Liguo, *et al*. 1994. Structural styles of the Longmenshan thrust belt and evolution of the foreland basin in western Sichuan Province, China[J]. Acta Geologica Sinica—English Edition, 7(4): 351~372.

Liu Shugen, Li Zhiwu, Sun Wei, *et al*. 2011. Basic characteristics of hydrocarbon-bearing stacked basins in Sichuan [J]. Geoscience, 46(1): 233~257 (in Chinese with English abstract).

Lu Songnian, Li Huaikun, Chen Zhihong, *et al*. 2004. Relationship between Neoproterozoic cratons of China and the Rodinia[J]. Earth Science Frontiers, 11(2): 515~523(in Chinese with English abstract).

Luo Hongwei. 2019. Source Analysis of the Xiaoheba Formation of the Silurian in Southeastern Sichuan[D]. Chengdu University of Technology (in Chinese with English abstract).

Ma Jun and Tao Yan. 2017. A preliminary exploration of the sediment source of the Xuanwei Formation strata in western Guizhou[C]//National Symposium on Mineral Formation Theory and Mineral Search Methods(in Chinese with English abstract).

Ma Yongsheng. 2009. Sequence Stratigraphy and Palaeogeography of South China[M]. Beijing: Science Press(in Chinese with English abstract).

Ma Yuxiao, Ji Xiangtian, Wang Hongfeng, *et al*. 2002. The Baguanhe Formation of Upper Sinian in the Panzhihua Area, Sichuan[J]. Mineralogy and Petrology, (4): 12~15 (in Chinese with English abstract).

McLennan S M, Hemming S, McDaniel D K, *et al*. 1993. Geochemical approaches to sedimentation, provenance, and tectonics[J]. Geological Society of America (Special Papers), 284: 21~40.

McLennan S M and Taylor S R. 1980. Th and U in sedimentary rocks: Crustal evolution and sedimentary recycling[J]. Nature, 285: 621~624.

Mclennan S M and Taylor S R. 1991. Sedimentary rocks and crustal evolution: Tectonic setting and secular trends [J]. The Journal of Geology, 99(1): 1~21.

Mei Mingxiang, Yang Fengjie, Gao Jinhan, *et al*. 2008. Glauconites formed in the high-energy shallow-marine environment of the Late Mesoproterozoic: Case study from Tieling Formation at Jixian Section in Tianjin, North China[J]. Earth Science Frontiers, 15(4): 146~158 (in Chinese with English abstract).

Mei Qinghua, He Dengfa, Wen Zhu, *et al*. 2014. Geologic structure and tectonic evolution of Leshan-Longnvsi paleo-uplift in Sichuan Basin, China[J]. Acta Petrolei Sinica, 35(1): 11~25 (in Chinese with English abstract).

Nesbitt H W and Markovics G. 1997. Weathering of granodioritic crust, long-term storage of elements in weathering profiles, and petrogenesis of siliciclastic sediments[J]. Geochimica et Cosmochimica Acta, 61(8): 1 653~1 670.

Nesbitt H W and Young G M. 1982. Early Proterozoic climates and plate motions inferred from major element chemistry of lutites[J]. Nature, 299: 715~717.

Nesbitt H W and Young G M. 1984. Prediction of some weathering trends of plutonic and volcanic rocks based on thermodynamic and kinetic considerations[J]. Geochimica et Cosmochimica Acta, 48: 1 523~1 534.

Odin G S and Matter A. 1981. De glauconiarum origine[J]. Sedimentology, 28(5): 611~641.

Pan Jiangtao, Liu Honghao, Yuan Yongsheng, *et al*. 2022. Late Permian Xuanwei Formation tuff from the western margin of the Upper Yangtze: Constraints on volcanic activity and Paleotethyan arc volcanism in the Emeishan Large Igneous Province[J]. Acta Geologica Sinica, 96(6): 1 985~2 000(in Chinese with English abstract).

Pang Pan. 2015. Three-dimensional Modeling and Tectonic Interpretation of the Emei Mountain Teaching Practice Area (Huangwan Area) [D]. Chengdu University of Technology (in Chinese with English abstract).

Pettijohn F J, Potter P E and Siever R. 1987. Sand and Sandstones(2nd edition)[M]. New York: Springer Verlag, 553.

Qi L, Hu J and Gregoire D C. 2000. Determination of trace elements in granites by inductively coupled plasma mass spectrometry[J]. Talanta, 51(3): 507~513

Qian Yi, Yu Wen, Liu Diyong, *et al*. 1984. Re-examination of the Aurignacian-Cambrian boundary section at Meishu Village, Jinning, Yunnan[J]. Science Bulletin, (15): 928~931(in Chinese with English abstract).

Qiu Y M, Gao S, McNaughton N J, *et al*. 2000. First evidence of >3.2 Ga continental crust in the Yangtze craton of south China and its implications for Archean crustal evolution and Phanerozoic tectonics[J]. Geology, 28: 11~14.

Que Wei. 2008. Trace Element Geochemical Characterization of the Permian-Triassic Boundary Stratigraphy on the Western Margin of the Yangzi Platform[D]. Chengdu University of Technology(in Chinese with English abstract).

Rimmer S, Thompson J, Goodnight S, *et al*. 2004. Multiple controls on the preservation of organic matter in Devonian-Mississippian marine black shales: Geochemical and petrographic evidence[J]. Palaeogeography Palaeoclimatology Palaeoecology, 215(1~2): 125~154.

Roser B P and Korsch R J. 1986. Determination of tectonic setting of sandstone-mudstone suites using content and ratio[J]. The Journal of Geology, 94(5): 635~650.

Rudnick R and Gao S. 2003. Composition of the continental crust[C]// Treatise on Geochemistry. Elsevier Ltd., 3: 1~64.

Shao Longyi, Gao Caixia, Zhang Chao, *et al*. 2013. Sequence-Palaeogeography and coal aaccumulation of Late Permian in southwestern China[J]. Acta Sedimentologica Sinica, 31(5): 856~866(in Chinese with English abstract).

Shellnutt J G. 2014. The Emeishan large igneous province: A synthesis [J]. Geoscience Frontiers, 5(3): 369~394.

Sun S S and McDonough W F. 1989. Chemical and isotopic systematics of oceanic basalts: Implications for mantle composition and processes [J]. Geological Society, London, Special Publications, 42(1): 313

~345.

Sun W H, Zhou M F, Yan D P, *et al*. 2008. Provenance and tectonic setting of the Neoproterozoic Yanbian Group, western Yangtze block (SW China)[J]. Precambrian Research, 167(1~2): 213~236.

Tan Cong, Yuan Xuanjun, Yu Bingsong, *et al*. 2019. Geochemical characteristics and paleoclimatic implications of the Upper Permian and Middle-Lower Triassic strata in southern Ordos Basin[J]. Geoscience, 33(3): 615~628(in Chinese with English abstract).

Taylor S R and Mclennan S M. 1985. The continental crust: Its composition and evolution[J]. The Journal of Geology, 94(4): 57~72.

Tian Jingchun and Zhang Xiang. 2016. Sedimentary Geochemistry[M]. Beijing: Geological Publishing House (in Chinese with English abstract).

Tian Ye. 2018. Petrographic Paleogeography of the Upper Permian Wujiaping Stage in the Sichuan Basin[D]. China University of Geosciences (Beijing) (in Chinese with English abstract).

Ukstins Peate I and Bryan S E. 2008. Re-evaluating plume-induced uplift in the Emeishan large igneous province[J]. Nature Geoscience, 1(9): 625~629.

Verma S P and Armstrong-Altrin J S. 2013. New multi-dimensional diagrams for tectonic discrimination of siliciclastic sediments and their application to Precambrian basins[J]. Chemical Geology, 355: 117~133.

Verma S P and Armstrong-Altrin J S. 2016. Geochemical discrimination of siliciclastic sediments from active and passive margin settings[J]. Sedimentary Geology, 332: 1~12.

Wang B, Wang L, Chen J, *et al*. 2014. Triassic three-stage collision in the Paleo-Tethys: Constraints from magmatism in the Jiangda-Deqen-Weixi continental margin arc, SW China[J]. Gondwana Research, 26(2): 475~491.

Wang Bei. 2017. Aurignacian-Early Cambrian Multi-screen Rifting in the Central Sichuan Basin and Its Genesis Mechanism[D]. China University of Geosciences (Beijing) (in Chinese with English abstract).

Wang Zecheng. 2002. Tectonic Sequence and Natural Gas Exploration in the Sichuan Basin[M]. Beijing: Geological Publishing House, 1~287(in Chinese with English abstract).

Willis K M, Stern R J and Clauer N. 1988. Age and geochemistry of Late Precambrian sediments of the Hammamat Series from the Northeastern Desert of Egypt[J]. Precambrian Research, 42(1~2): 173~187.

Wu Chaodong, Yang Chengyun and Chen Qiying. 1999. The origin and geochemical characteristics of Upper Sinain-Lower Cambrian black shales in western Hunan[J]. Acta Petrologica et Mineralogica, 18(1): 26~39(in Chinese with English abstract).

Xiao Jiafei. 2005. The evolution of the Mid-Proterozoic-Triassic sedimentary basin and the element geochemical background of strata at the SW of the Yangtze Block (Ph. D. dissertation) [D]. Guiyang: Chinese Academy of Sciences (in Chinese with English abstract).

Xiao L, Xu Y, Mei H, *et al*. 2004. Distinct mantle sources of low-Ti and high-Ti basalts from the western Emeishan large igneous province, SW China: Implications for plume-lithosphere interaction[J]. Earth and Planetary Science Letters, 228: 525~546.

Xiong Shunhua and Li Jianlin. 1984. The characteristics about the basalt in the edge of continental rift of late Permian in the Emei mountain [J]. Journal of Chengdu Institute of Geology, 1(3): 43~59,123~124, 134~135 (in Chinese).

Xiong Xiaohui and Xiao Jiafei. 2011. Geochemical indicators of sedimentary environments—A summary[J]. Earth and Environment, 39(3): 405~414 (in Chinese with English abstract).

Xu Y, Chung S L, Jahn B, *et al*. 2001. Petrologic and geochemical constraints on the petrogenesis of Permian-Triassic Emeishan flood basalts in southwestern China[J]. Lithos, 58(3~4): 145~168.

Xu Yigang, He Bin, Luo Zhenyu, *et al*. 2013. Study on mantle and large igneous provinces in China: An overview and perspectives[J]. Bulletin of Mineralogy, Petrology and Geochemistry, 32(1): 25~39(in Chinese with English abstract).

Yang J, Cawood P A and Du Y. 2015. Voluminous silicic eruptions during late Permian Emeishan igneous province and link to climate cooling[J]. Earth and Planetary Science Letters, 432: 166~175.

Yao Jie. 2018. Study on the Reservoir Properties of the Lower Triassic Feixianguan Formation in the Longmen Cave Section of Emeishan [D]. Chengdu University of Technology (in Chinese with English abstract).

Yin A and Harrison T M. 2000. Geologic evolution of the Himalayan-Tibetan orogen[J]. Annual Review of Earth and Planetary Sciences, 28(1): 211~280.

Yu Shihua. 2016. Source Analysis of the Late Triassic Sujiahe Formation in the Western Sichuan Basin and Its Tectonic Significance[D]. University of Chinese Academy of Sciences(Guangzhou Institute of Geochemistry, Chinese Academy of Sciences) (in Chinese with English abstract).

Yu Xin, Yang Jianghai, Liu Jianzhong, *et al*. 2017. Provenance of the Late Permian Longtan Formation in SW Guizhou Province and implication for reconstruction of regional sedimentation and paleogeography [J]. Acta Geologia Sinica, 91(6): 1 374~1 385(in Chinese with English abstract).

Zeng Yunfu, Shen Lijuan, Li Shilin, *et al*. 1979. Preliminary understanding of the late Aurignacian and Early Cambrian sedimentary environment of Emei Mountain[J]. Journal of Chengdu Geological Institute, (1): 68~72 (in Chinese with English abstract).

Zhang H, Cao C Q, Liu X L, *et al*. 2016. The terrestrial end-Permian mass extinction in South China[J]. Palaeogeogr. Palaeoclimatol. Palaeoecol., 448: 108~124.

Zhang Haoran, Jiang Hua, Chen Zhiyong, *et al*. 2020. A review of the research status of Caledonian movement stages in Sichuan Basin and surrounding areas[J]. Bulletin of Geological Science and Technology, 39(5): 118~126(in Chinese with English abstract).

Zhang Jiqing. 1983. Rock types and the analysis of their sedimentary facies of the Lower and Middle Triassic section in Longmendong, Emei, Sichuan (in Chinese with English abstract): Bulletin of the Chengdu Institute of Geology and Mineral Resources[J]. Chinese Academy of Geological Sciences, 1: 1~50 (in Chinese with English abstract).

Zhang Tianfu, Sun Lixin, Zhang Yun, *et al*. 2016. Geochemical characteristics of the Jurassic Yan'an and Zhiluo formations in the northern margin of Ordos Basin and their paleoenvironmental implications[J]. Acta Geologica Sinica, 90(12): 3 454~3 472 (in Chinese with English abstract).

Zhang Tingshan, He Yingxie, Wu Kunyu, *et al*. 2017. Sedimentary facies and controlling factors of coal accumulation of the Upper Permian Xuanwei Formation in Junlian area[J]. Lithologic Reservoirs, 29 (1): 1~10 (in Chinese with English abstract).

Zhang Yueqiao, Dong Shuwen, Li Jianhua, *et al*. 2011. Mesozoic multidirectional compressional tectonics and formation-reformation of Sichuan basin[J]. Geology in China, 38(2): 233~250(in Chinese with English abstract).

Zhang Z, Qin J, Lai S, *et al*. 2020. Origin of Late Permian amphibole syenite from the Panxi area, SW China: High degree fractional crystallization of basaltic magma in the inner zone of the Emeishan mantle plume[J]. International Geology Review, 62(2): 210~224.

Zhang Zhaochong. 2009. A discussion on some important problems concerning the Emeishan large igneous province[J]. Geology in China, 36(3): 634~646 (in Chinese with English abstract).

Zhang Z W, Yang X Y, Li S, *et al*. 2010. Geochemical characteristics of the Xuanwei Formation in West Guizhou: Significance of sedimentary environment and mineralization[J]. Chinese Journal of Geochemistry, 29(4): 355~364.

Zhao G, Wang Y, Huang B, *et al*. 2018. Geological reconstructions of the East Asian blocks: From the breakup of Rodinia to the assembly of Pangea[J]. Earth-Sci. Rev, 186: 262~286.

Zhao L X, Dai S F, Graham I T, *et al*. 2016. New insights into the lowest Xuanwei Formation in eastern Yunnan Province, SW China: Implications for Emeishan large igneous province felsic tuff deposition and the cause of the end-Guadalupian mass extinction[J]. Lithos, 264: 375~391.

Zhao L X, Dai S F, Graham I T, *et al*. 2017. Cryptic sediment-hosted critical element mineralization from eastern Yunnan Province, southwestern China: Mineralogy, geochemistry, relationship to Emeishan alkaline magmatism and possible origin[J]. Ore Geology Reviews, 80: 116~140.

Zhao J H and Zhou M F. 2008. Neoproterozoic adakitic plutons in the northern margin of the Yangtze Block, China: Partial melting of a thickened lower crust and implications for secular crustal evolution [J]. Lithos, 104(1~4): 231~248.

Zhao Zongju, Zhou Hui, Chen Xuan, *et al*. 2012. Sequence lithofacies paleogeography and favorable exploration zones of the Permian in Sichuan Basin and adjacent areas, China[J]. Acta Petrolei Sinica, 33 (S2): 35~51(in Chinese with English abstract).

Zheng J P, Griffin W L, Suzanne Y, *et al*. 2006. Widespread Archean basement beneath the Yangtze Craton[J]. Geology, 34: 417~420.

Zheng Rongcai, Dai Chaocheng, Zhu Rukai, *et al*. 2009. Sequence-based lithofacies and paleogeographic characteristics of Upper Triassic Xujiahe Formation in Sichuan Basin[J]. Geological Review, 55(4): 484~495 (in Chinese with English abstract).

Zhong Y, He B, Mundil R, *et al*. 2014. CA-TIMS zircon U-Pb dating of felsic ignimbrite from the Binchuan section: Implications for the termination age of Emeishan large igneous province[J]. Lithos, 204: 14~19.

Zhou L, Zhang Z, Li Y, *et al*. 2013. Geological and geochemical characteristics in the paleo-weathering crust sedimentary type REE deposits, western Guizhou, China[J]. Journal of Asian Earth Sciences, 73 (sep. 5): 184~198.

Zhu B, Guo Z, Zhang S, *et al*. 2019. What triggered the early-stage eruption of the Emeishan large igneous province? [J]. GSA Bulletin, 131(11~12): 1 837~1 856.

Zhu B, Guo Z, Zhang S, *et al*. 2021. Low-Ti gabbroic pluton in Dali, SW China: New evidence for back-arc lithospheric melting inducing early-stage magmatism of the Emeishan large igneous province[J]. Journal of the Geological Society, 178(6): 1~13.

Zhu Jiang, Zhang Zhaochong, Hou Tong, *et al*. 2011. LA-ICP-MS zircon U-Pb geochronology of the tuffs on the uppermost of the Emeishan basalt succession in Panxian county, Guizhou Province: Constraints on genetic link between Emeishan large igneous province and the mass extinction[J]. Acta Petrologica Sinica, 27(9): 2 743~2 751 (in Chinese with English abstract).

Zhu M, Chen H, Yu L, *et al*. 2018. Provenance of the Early Triassic in the southwestern Sichuan Basin, Upper Yangtze, and its implications for tectonic evolution[J]. Canadian Journal of Earth Sciences, 55(1): 70~83.

Zhu M, Chen L H, Yu L, *et al*. 2017. Provenance of the Early Triassic in the southwestern Sichuan Basin, Upper Yangtze, and its implications for tectonic evolution[J]. Canadian Journal of Earth Sciences, cjes-2017-0092.

Zhu Zhijun and Chen Hongde. 2012. An analysis of sedimentary characteristics and model of Silurian Xiaoheba Formation in southeastern Sichuan Province[J]. Geology in China, 39(1): 64~76(in Chinese with English abstract).

Zi J W, Cawood P A, Fan W M, *et al*. 2012. Triassic collision in the Paleo-Tethys Ocean constrained by volcanic activity in SW China[J]. Lithos, 144: 145~160.

附中文参考文献

陈 斌, 李 勇, 王伟明, 等. 2016. 晚三叠世龙门山前陆盆地须家河组物源及构造背景分析[J]. 地质学报, 90(5): 857~872.

陈风霖, 谢 渊, 崔晓庄, 等. 2018. 扬子西缘峨边群玄武岩年代学、地球化学特征及构造意义[J]. 矿物岩石, 38(3): 76~86.

陈建平, 李 伟, 倪云燕, 等. 2018. 四川盆地二叠系烃源岩及其天然气勘探潜力(一)——烃源岩空间分布特征[J]. 天然气工业, 38(5): 1~16.

陈 璐. 2014. 四川峨眉地区上白垩统夹关组遗迹组构研究[D]. 成都:西南石油大学.

陈淑慧, 李 云, 胡作维, 等. 2014. 海绿石的成因、指相作用及其年龄意义[J]. 岩石矿物学杂志, 33(5): 971~979.

陈宗清. 2011. 论四川盆地二叠系乐平统龙潭组页岩气勘探[J]. 天然气技术与经济, 5(2): 21~26,78.

邓江红. 2013. 峨眉山地质认识实习教程[M]. 北京: 地质出版社.

邓旭升. 2019. 右江盆地北缘上二叠统沉积相和沉积物源分析[D]. 中国地质大学.

邓煜霖, 郎兴海, 崔志伟, 等. 2018. 四川江油马角坝剌林包剖面二叠-三叠系间粘土岩研究[J]. 岩石矿物学杂志, 237(3): 417~433.

杜利林, 郭敬辉, 耿元生, 等. 2013. 扬子西南缘盐边群时代及构造环境: 来自碎屑沉积的约束[J]. 岩石学报, 29(2): 641~672.

冯 冲, 邹华耀, 郭彤楼. 2015. 四川盆地晚二叠世-早三叠世沉积演化及其对天然气富集的意义[J]. 地球科学与环境学报, 37(4): 44~53.

高彩霞. 2015. 川渝滇黔晚二叠世层序-古地理与聚煤规律研究[D]. 中国矿业大学(北京).

高莲凤, 周 巍, 张 盈, 等. 2017. 藏南贡嘎晚侏罗世-早白垩世海相地层地球化学特征与古海洋环境演化[J]. 地学前缘, 24(1): 195~204.

耿元生, 旷红伟, 柳永清, 等. 2017. 扬子地块西、北缘中元古代地层的划分与对比[J]. 地质学报, 91(10): 2 151~2 174.

何冰辉. 2015. 峨眉山大火成岩省构造活动的上二叠统宣威组地层记录[D]. 中国地质大学(北京).

何冰辉, 刘少峰, 吴 鹏. 2017. 滇东者海上二叠统宣威组下部地层碎屑锆石 U-Pb 测年及其地质意义[J]. 地质调查与研究, 40(2): 126~133, 146.

胡瑞忠, 陶 琰, 钟 宏, 等. 2005. 地幔柱成矿系统: 以峨眉山地幔柱为例[J]. 地学前缘, 12(1): 42~54.

黄 丹. 2012. 四川盆地西部上二叠统长兴组-下三叠统飞仙关组层序地层学研究[D]. 荆州: 长江大学.

蒋晓丽, 龚大兴, 周家云, 等. 2022. 滇黔相邻区二叠系宣威组富稀土黏土岩综合研究进展[J]. 矿产综合利用,(1): 32~41.

焦 鑫, 柳益群, 杨 晚, 等. 2017. 水下火山喷发沉积特征研究进展[J]. 地球科学进展, 32(9): 926~936.

赖旭龙, 孙亚东, 江海水. 2009. 峨嵋山大火成岩省火山活动与中、晚二叠世之交生物大灭绝[J]. 中国科学基金, (6): 353~356.

李 宸, 郎兴海, 邓煜霖, 等. 2020. 四川盆地峨眉山雷口坡组底部黏土岩(绿豆岩)的年代学及地球化学特征[J]. 矿物岩石地球化学通报, 39(4): 810~825.

李明龙, 郑德顺, 戴光忠, 等. 2014. 豫西济源盆地侏罗系泥质岩地球化学特征及其环境和物源示踪[J]. 地质学报, 88(2): 228~238.

梁狄刚, 郭彤楼, 边立曾, 等. 2009. 中国南方海相生烃成藏研究的若干新进展(三) 南方四套区域性海相烃源岩的沉积相及发育的控制因素[J]. 海相油气地质, (2): 1~19.

梁新权, 周 云, 蒋 英, 等. 2013. 二叠纪东吴运动的沉积响应差异: 来自扬子和华夏板块吴家坪组或龙潭组碎屑锆石 LA-ICPM-SU-Pb 年龄研究[J]. 岩石学报, 29(10): 3 592~3 606.

林茂炳. 1994. 初论龙门山推覆构造带的基本结构样式[J]. 成都理工学院学报, 21(3): 1~7.

刘和甫, 梁慧社, 蔡立国, 等. 1994. 川西龙门山冲断系构造样式与前陆盆地演化[J]. 地质学报, 68(2): 101~118.

刘树根，李智武，孙　玮，等. 2011. 四川含油气叠合盆地基本特征[J]. 地质科学，46(1)：233～257.

陆松年，李怀坤，陈志宏，等. 2004. 新元古时期中国古大陆与罗迪尼亚超大陆的关系[J]. 地学前缘，11(2)：515～523.

罗宏谓. 2019. 川东南志留系小河坝组物源分析[D]. 成都理工大学.

马　骏，陶　琰. 2017. 贵州西部地区宣威组地层沉积物源初探[A]. 全国成矿理论与找矿方法学术讨论会[C].

马永生. 2009. 中国南方层序地层与古地理[M]. 北京：科学出版社.

马玉孝，纪相田，王洪峰，等. 2002. 四川攀枝花地区的上震旦统把关河组[J]. 矿物岩石，(4)：12～15.

梅冥相，杨锋杰，高金汉. 等. 2008. 中元古代晚期浅海高能沉积环境中的海绿石：以天津蓟县剖面铁岭组为例[J]. 地学前缘，15(4)：146～158.

梅庆华，何登发，文　竹，等. 2014. 四川盆地乐山-龙女寺古隆起地质结构及构造演化[J]. 石油学报，35(1)：11～25.

潘江涛，刘红豪，袁永盛，等. 2022. 上扬子西缘晚二叠世宣威组凝灰岩：对峨眉山大火成岩省火山活动及古特提斯弧火山作用的约束[J]. 地质学报，96(6)：1 985～2 000.

庞　攀. 2015. 峨眉山教学实习区(黄湾地区)三维建模及构造解译[D]. 成都理工大学.

钱　逸，余　汶，刘第镛，等. 1984. 云南晋宁梅树村震旦系-寒武系界线剖面再研究[J]. 科学通报，(15)：928～931.

阙　薇. 2008. 扬子地台西缘二叠—三叠系界线地层微量元素地球化学特征研究[D]. 成都理工大学.

邵龙义，高彩霞，张　超，等. 2013. 西南地区晚二叠世层序-古地理及聚煤特征[J]. 沉积学报，31(5)：856～866.

谭　聪，袁选俊，于炳松，等. 2019. 鄂尔多斯盆地南缘上二叠统—中下三叠统地球化学特征及其古气候、古环境指示意义[J]. 现代地质，33(3)：615～628.

田景春，张　翔. 2016. 沉积地球化学[M]. 北京：地质出版社.

田　野. 2018. 四川盆地上二叠统吴家坪期岩相古地理研究[D]. 中国地质大学(北京).

王　贝. 2017. 四川盆地中部震旦纪—早寒武世多幕裂陷作用及其成因机制[D]. 中国地质大学(北京).

汪泽成. 2002. 四川盆地构造层序与天然气勘探[M]. 北京：地质出版社，1～287.

吴朝东，杨承运，陈其英. 1999. 湘西黑色岩系地球化学特征和成因意义[J]. 岩石矿物学杂志，18(1)：26～39.

肖加飞. 2015. 扬子地块西南缘中元古代—三叠纪沉积盆地演化及地层的元素地球化学背景[D]. 贵阳：中国科学院研究生院(地球化学研究所).

熊舜华，李建林. 1984. 峨眉山区晚二叠世大陆裂谷边缘玄武岩系的特征[J]. 成都地质学院学报，1(3)：43～59，123～124，134～135.

熊小辉，肖加飞. 2011. 沉积环境的地球化学示踪[J]. 地球与环境，39(3)：405～414.

徐义刚，何　斌，罗震宇，等. 2013. 我国大火成岩省和地幔柱研究进展与展望[J]. 矿物岩石地球化学通报，32(1)：25～39.

姚　婕. 2018. 峨眉山龙门洞剖面下三叠统飞仙关组储层物性研究[D]. 成都理工大学.

余世花. 2016. 四川盆地西部晚三叠世须家河组物源分析及其构造意义[D]. 中国科学院大学(中国科学院广州地球化学研究所).

于　鑫，杨江海，刘建中，等. 2017. 黔西南晚二叠世龙潭组物源分析及区域沉积古地理重建[J]. 地质学报，91(6)：1 374～1 385.

曾允孚，沈丽娟，李世麟，等. 1979. 对峨眉山震旦纪晚期及寒武纪早期的沉积环境的初步认识[J]. 成都地质学院学报，(1)：68～72.

张浩然，姜　华，陈志勇，等. 2020. 四川盆地及周缘地区加里东运动幕次研究现状综述[J]. 地质科技通报，39(5)：118～126.

张继庆. 1983. 四川峨眉龙门洞剖面中、下三叠统岩石特征及沉积相分析[J]. 中国地质科学院成都地质矿产研究所文集，(1)：1～50.

张天福，孙立新，张　云，等. 2016. 鄂尔多斯盆地北缘侏罗纪延安组、直罗组泥岩微量、稀土元素地球化学特征及其古沉积环境意义[J]. 地质学报，90(12)：3 454～3 472.

张廷山，何映颉，伍坤宇，等. 2017. 筠连地区上二叠统宣威组沉积相及聚煤控制因素[J]. 岩性油气藏，29(1)：1～10.

张岳桥，董树文，李建华，等. 2011. 中生代多向挤压构造作用与四川盆地的形成和改造[J]. 中国地质，38(2)：233～250.

张招崇. 2009. 关于峨眉山大火成岩省一些重要问题的讨论[J]. 中国地质，36(3)：634～646.

赵宗举，周　慧，陈　轩，等. 2012. 四川盆地及邻区二叠纪层序岩相古地理及有利勘探区带[J]. 石油学报，33(S2)：35～51.

郑荣才，戴朝成，朱如凯，等. 2009. 四川类前陆盆地须家河组层序-岩相古地理特征[J]. 地质论评，55(4)：484～495.

朱　江，张招崇，侯　通，等. 2011. 贵州盘县峨眉山玄武岩顶部凝灰岩 LA-ICP-MS 锆石 U-Pb 年龄：对峨眉山大火成岩省与生物大规模灭绝关系的约束[J]. 岩石学报，27(9)：2 743～2 751.

朱志军，陈洪德. 2012. 川东南地区早志留世晚期沉积特征及沉积模式分析[J]. 中国地质，39(1)：64～76.